Table of Contents

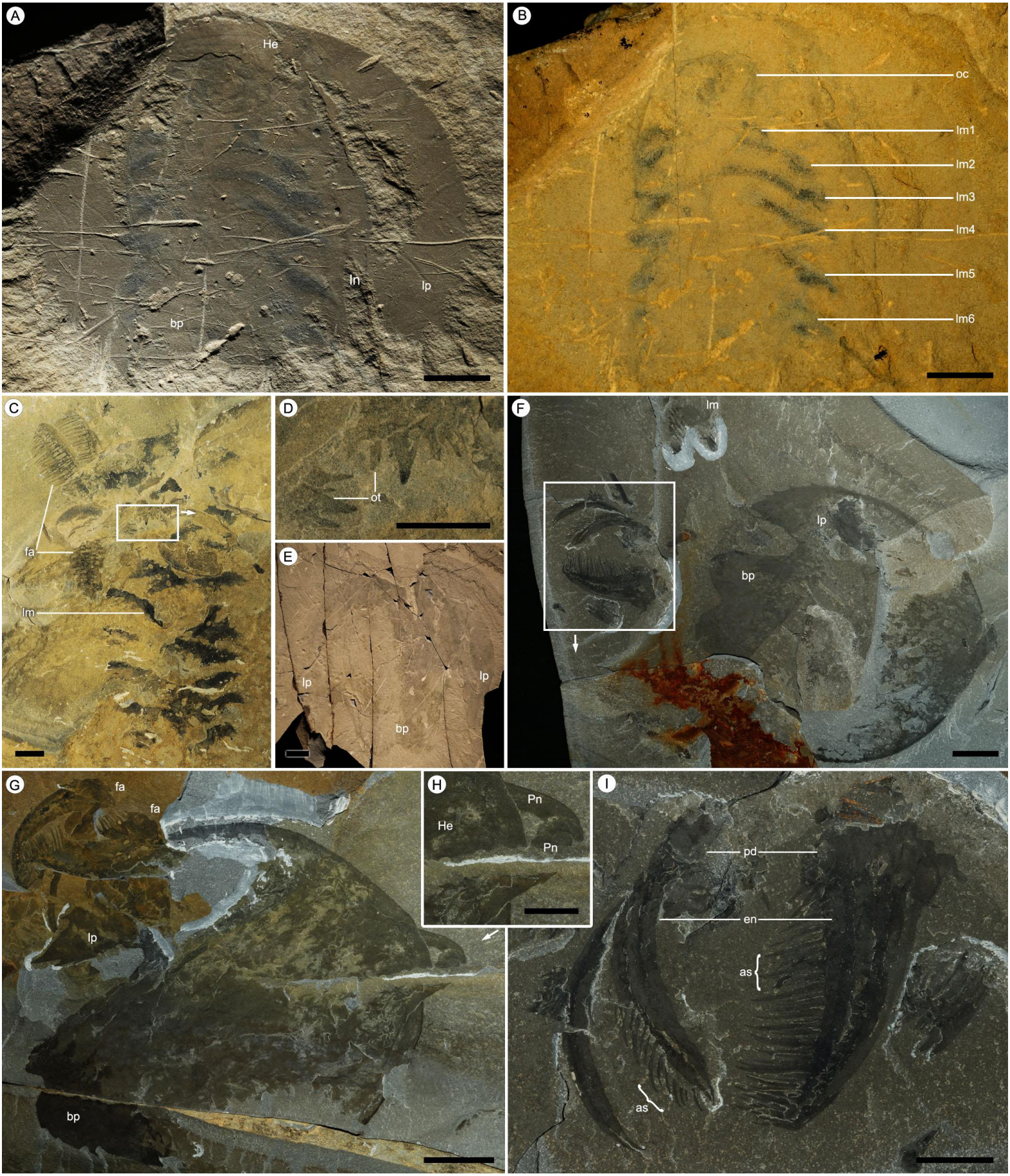
A
He
In
Ip
bp
B
oc
lm1
lm2
lm3
lm4
lm5
lm6
C
fa
lm
D
ot
E
Ip
Ip
bp
F
lm
Ip
bp
G
fa
fa
Ip
bp
H
Pn
He
Pn
I
pd
en
as
as

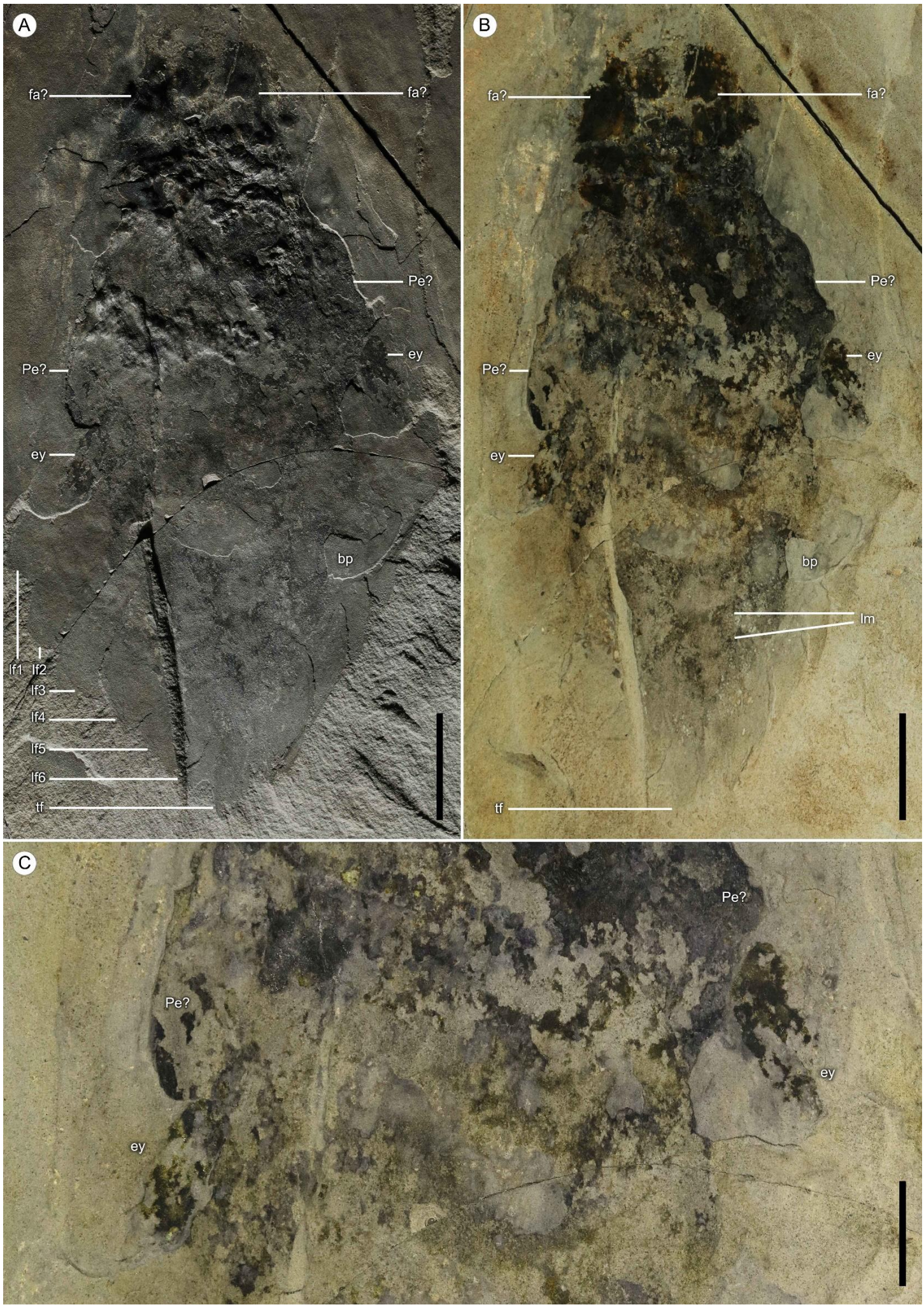
A
fa?
fa?
Pe?
ey
Pe?
ey
bp
lf1
lf2
lf3
lf4
lf5
lf6
tf
B
fa?
fa?
Pe?
ey
Pe?
ey
bp
lm
tf
C
Pe?
Pe?
ey
ey

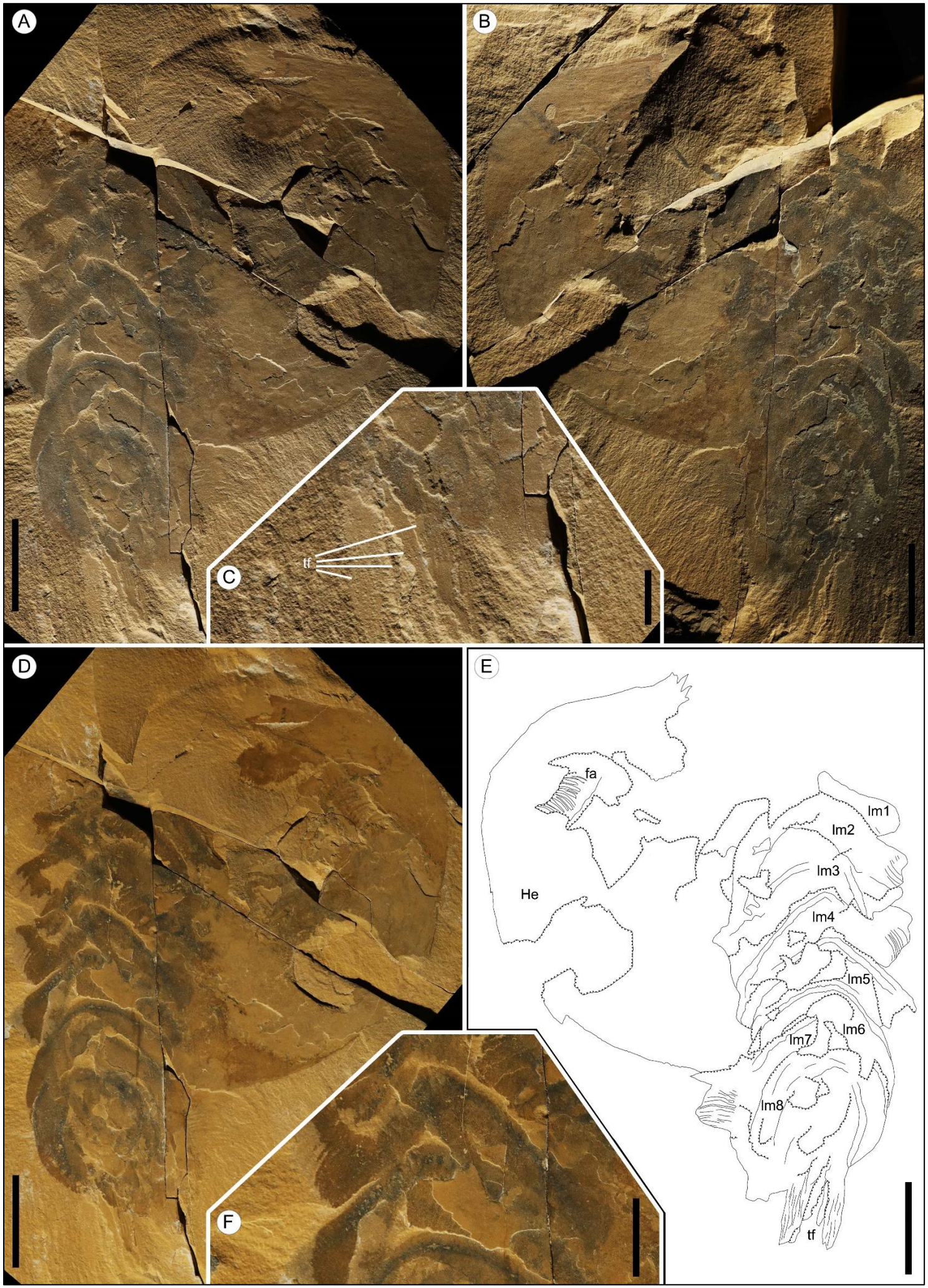

3

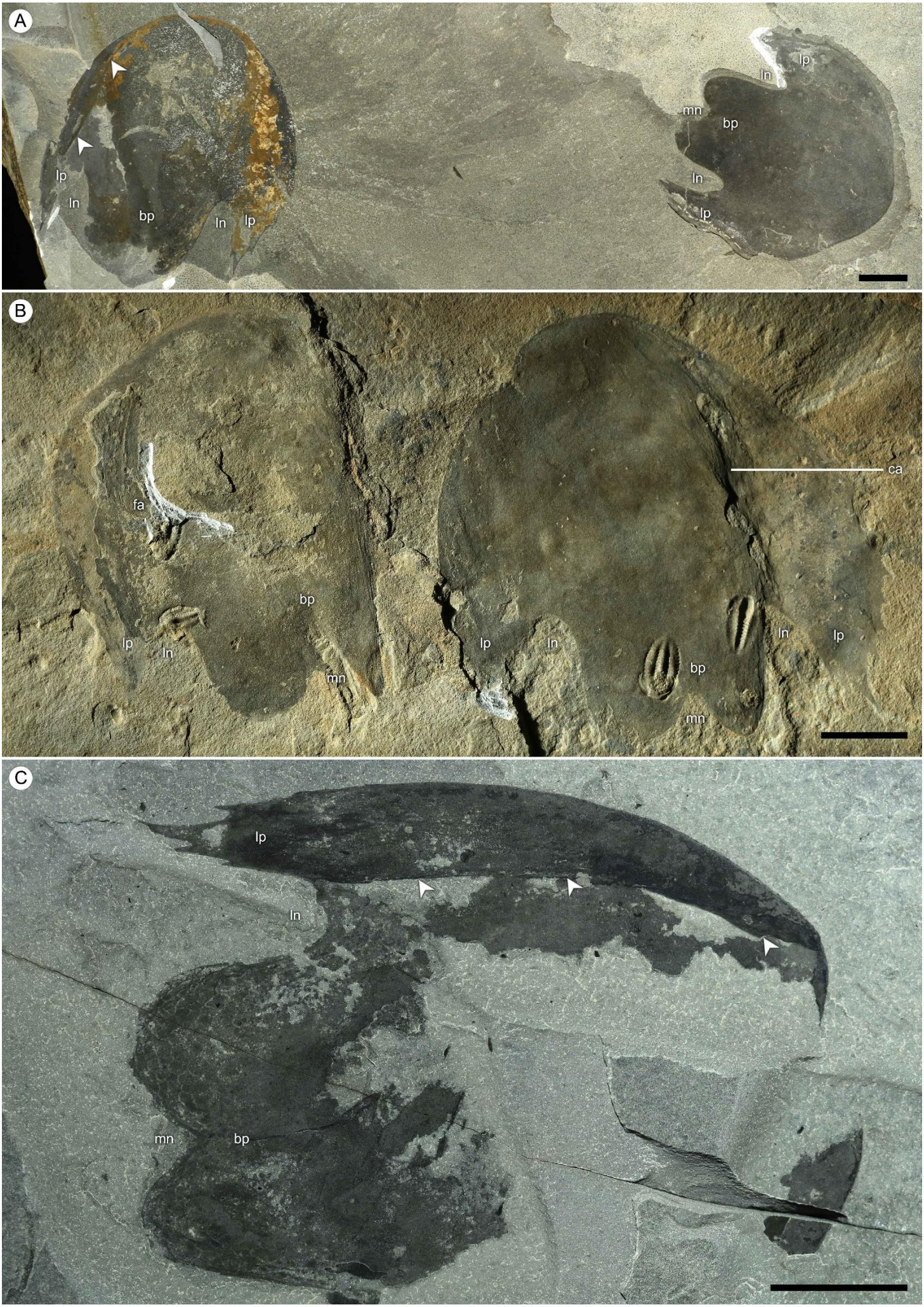
A
lp
ln
bp
ln
lp
lp
ln
mn
bp
ln
lp
B
fa
bp
lp
ln
mn
lp
ln
bp
mn
ln
lp
ca
C
lp
ln
mn
bp

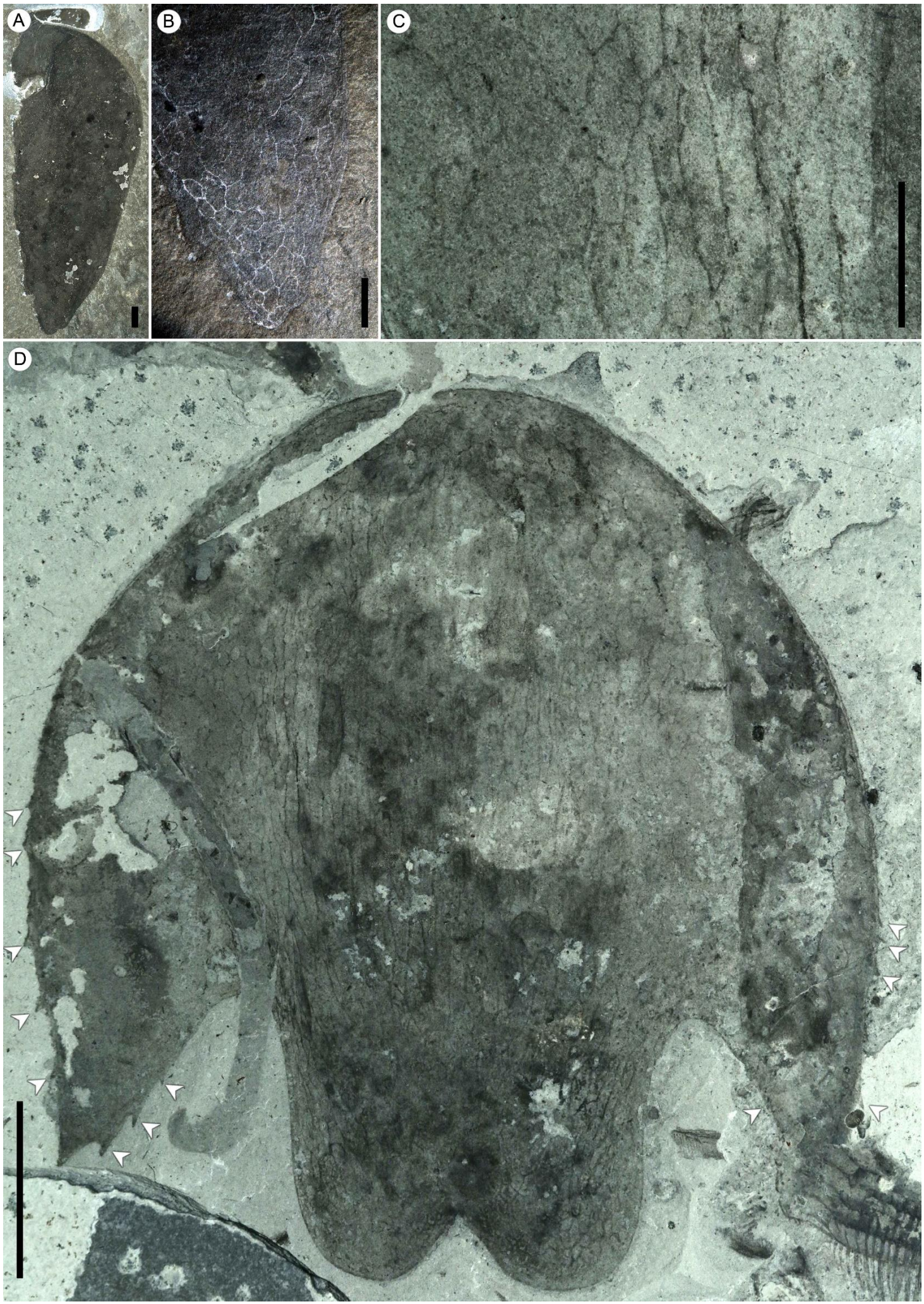

5

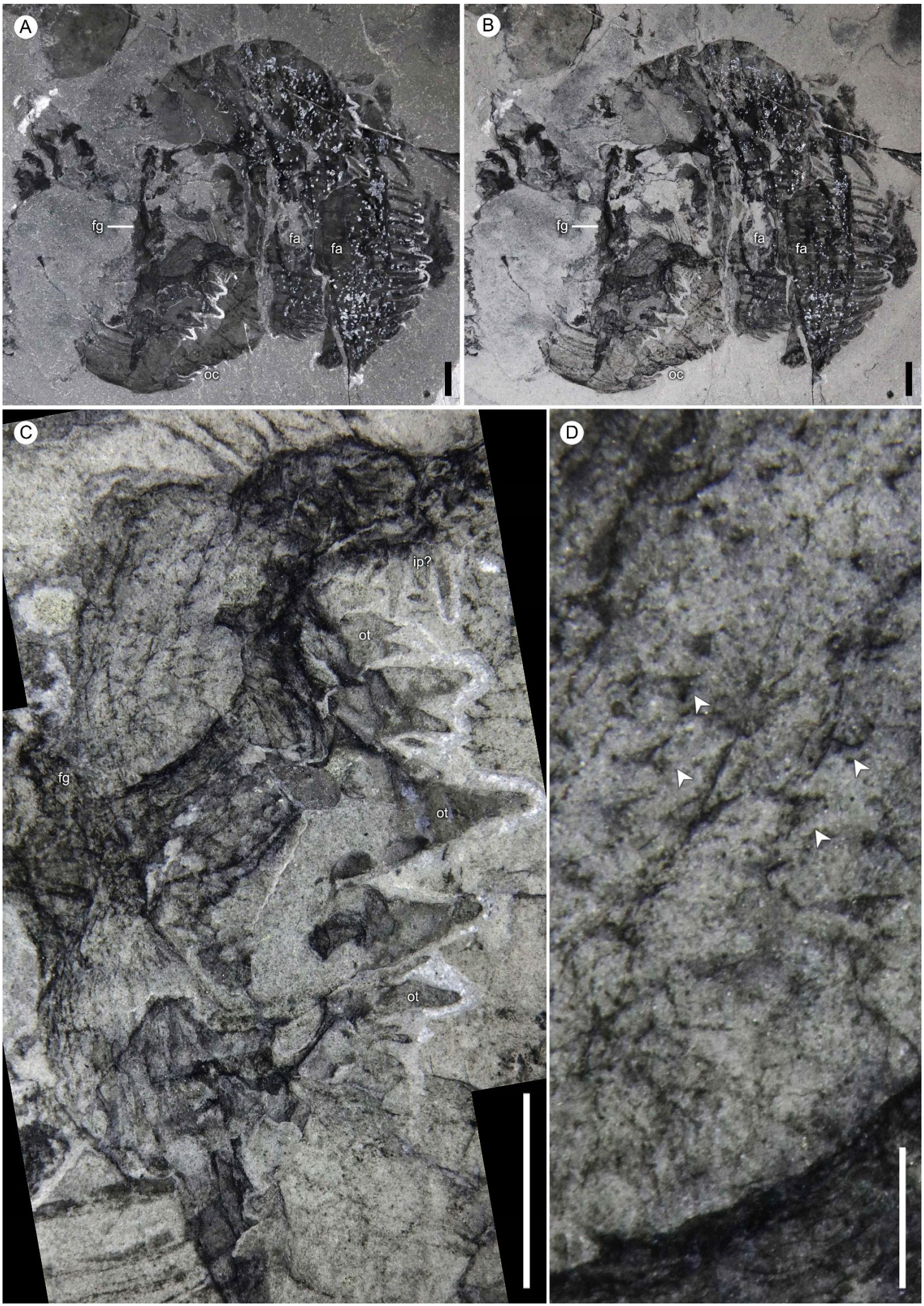
A
fg
fa
fa
oc
B
fg
fa
fa
oc
C
ip?
ot
fg
ot
ot
D

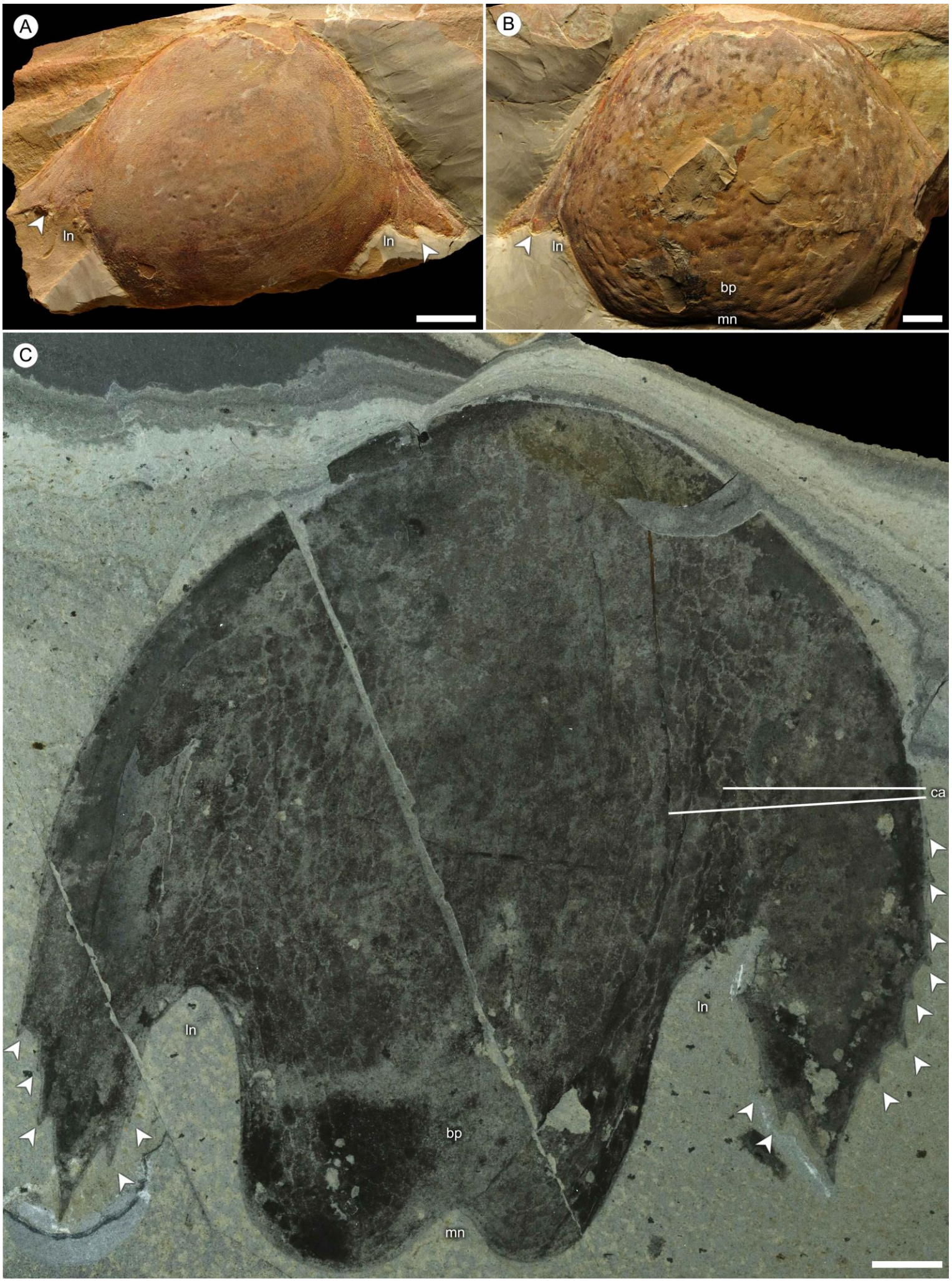
A
ln
ln
B
ln
bp
mn
C
ca
ln
ln
bp
mn

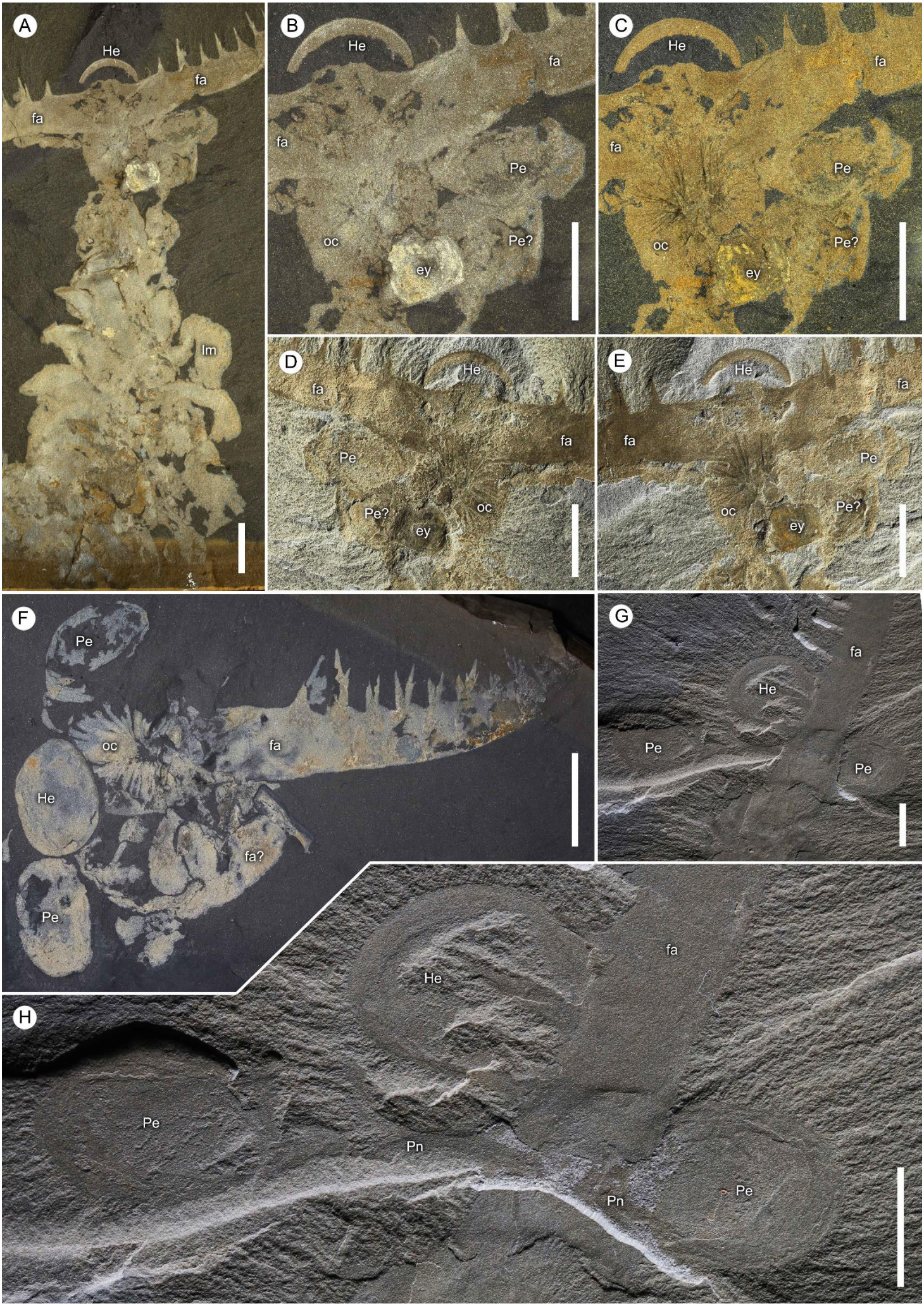
A
He
fa
fa
lm
B
He
fa
fa
Pe
oc
Pe?
ey
C
He
fa
fa
Pe
oc
Pe?
ey
D
He
fa
fa
Pe
Pe?
oc
ey
E
He
fa
fa
Pe
oc
Pe?
ey
F
Pe
oc
fa
He
fa?
Pe
G
fa
He
Pe
Pe
H
fa
He
Pe
Pn
Pn
Pe

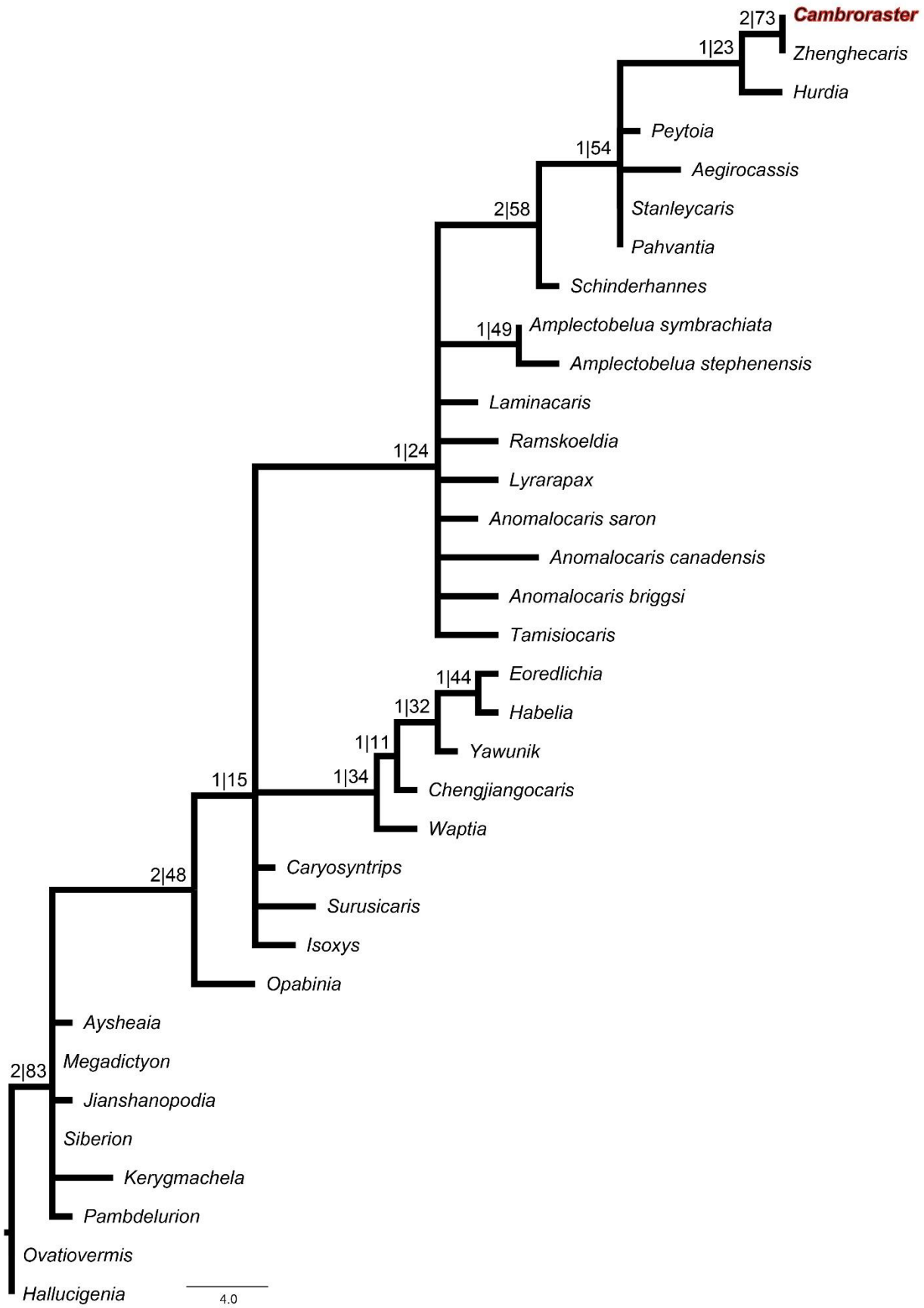
2|73
Cambroraster
1|23
Zhenghecaris
Hurdia
Peytoia
1|54
Aegirocassis
2|58
Stanleycaris
Pahvantia
Schinderhannes
1|49
Amplectobelua symbrachiata
Amplectobelua stephenensis
Laminacaris
Ramskoeldia
1|24
Lyrarapax
Anomalocaris saron
Anomalocaris canadensis
Anomalocaris briggsi
Tamisiocaris
1|44
Eoredlichia
1|32
Habelia
1|11
Yawunik
1|15
1|34
Chengjiangocaris
Waptia
2|48
Caryosyntrips
Surusicaris
Isoxys
Opabinia
Aysheaia
2|83
Megadictyon
Jianshanopodia
Siberion
Kerygmachela
Pambdelurion
Ovatiovermis
Hallucigenia
4.0

9

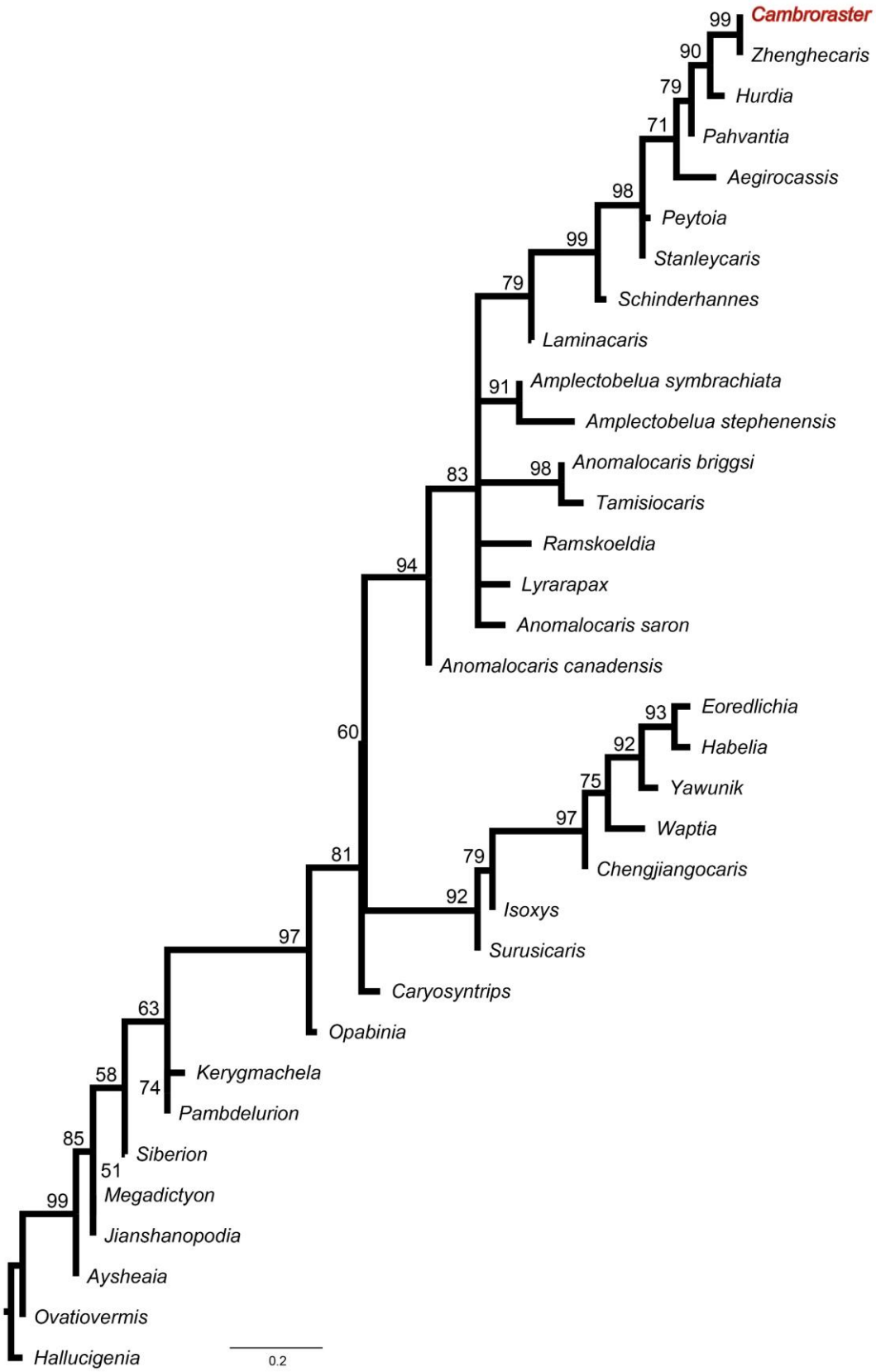
Cambroraster
Zhenghecaris
Hurdia
Pahvantia
Aegirocassis
Peytoia
Stanleycaris
Schinderhannes
Laminacaris
Amplectobelua symbrachiata
Amplectobelua stephenensis
Anomalocaris briggsi
Tamisiocaris
Ramskoeldia
Lyrarapax
Anomalocaris saron
Anomalocaris canadensis
Eoredlichia
Habelia
Yawunik
Waptia
Chengjiangocaris
Isoxys
Surusicaris
Caryosyntrips
Opabinia
Kerygmachela
Pambdelurion
Siberion
Megadictyon
Jianshanopodia
Aysheaia
Ovatiovermis
Hallucigenia
99
90
79
71
98
99
79
91
98
83
94
60
93
92
75
97
79
81
92
97
63
58
74
85
51
99
0.2

10

Supplementary Figure Captions

Page 1 – Supplementary Figure 1: Additional *Cambroraster* specimens. A,B, ROMIP 65088, showing 5-6 lamellar bands below H-element; A, photographed dry; B, photographed underwater, first 3-4 lamellar bands are anterior to the ln; C,D, ROMIP 65090, disarticulated body assemblage; C, overview; D, closeup of teeth on oral plates; E, ROMIP 65077, largest known specimen; F, ROMIP 65089, disarticulated assemblage; G,H, ROMIP 65091 disarticulated assemblage; G, overview; H, closeup of P-element necks; I, closeup of boxed area in F, showing pair of frontal appendages at differing burial angles. A-D,H,I bars=10mm; E-G bars=20mm. Abbreviations: lm#=lamellar band number, others as in Figs. 1-2.

Page 2 – Supplementary Figure 2: Additional photos of the holotype (ROMIP 65078 part). A, body, photographed dry; B, body, photographed underwater; C, closeup of eyes, photographed underwater. A,B bars=20mm; C, bar=10mm. Abbreviations as in Figs 1-2.

Page 3 – Supplementary Figure 3: Additional photos of ROMIP 65093. A,B, part and counterpart photographed dry; C, closeup of blades of tail fan, photographed dry; D, part photographed underwater; E, line drawing of part, mirrored horizontally; F, closeup of bands of lamellae, photographed underwater. A,B,D,E, bars=20mm; C, bar=5mm; F, bar=10mm. Abbreviations: lm#=lamellar band number, tf=tail fan, others as in Figs 1-2.

Page 4 – Supplementary Figure 4: Varying preservation of *Cambroraster* H-elements. A, ROMIP 65313, pair of H-elements in near horizontal orientation, specimen at left showing some overfolding of the lateral area (indicated by arrows); B, ROMIP 65314, pair of H-elements, showing compression artefacts and variations in the shape of the axial and lateral areas and the number of visible marginal spines, related to oblique burial angles (most extreme in the specimen at left); C, ROMIP 65315, H-element with narrow lateral area underlain by a dark band (arrows), with few marginal spines visible, suggesting overfolding of the edge of the sclerite. Bars=20mm. Abbreviations as in Figs 1-2.

Page 5 – Supplementary Figure 5: Reticulate pattern on *Cambroraster* carapace elements. A,B, ROMIP 65082, P-element; A, overview under cross polarized light; B, closeup under low angle light showing pattern; C,D, ROMIP 65079, H-element; C, closeup showing gradation from more rounded lateral cells (left) to elongate cells centrally (right); D, overview, arrows indicate spines on the lateral areas. A-C, bars=5mm; D, bar=20mm. Abbreviations as in Figs 1-2.

Page 6 – Supplementary Figure 6: Oral cone of *Cambroraster* (ROMIP 65083). A, photographed dry, showing both appendages and oral cone in lateral view, note hooked auxiliary spines; B, photographed underwater; C, closeup of circumoral teeth; D, closeup of denticles attached to wrinkled cuticle (arrows). A-C, bars=5mm; D, bar=1mm. Abbreviations as in Figs. 1-2.

Page 7 – Supplementary Figure 7: Comparison of *Cambroraster* and *Zhenghecaris*. A,B, *Zhenghecaris shankouensis*, photos courtesy of Fangchen Zhao; A, Nanjing Institute of Geology and Palaeontology (NIGPAS) 162519; B, NIGPAS 162520; C, *Cambroraster falcatus* H-element, ROMIP 65316. Arrows indicate spines adorning lateral areas; *Zhenghecaris* has only a single spine on the inner side of the posterolateral process. Bars=10mm. Abbreviations: ca=compression artefact, others as in Figs 1-2.

Page 8 – Supplementary Figure 8: Head carapace complex in *Anomalocaris canadensis*. A-E, ROMIP 51213; A, part, overview, B, part, closeup of head, direct light, showing highly reflective eye and less reflective sclerotized elements; C, part, cross polarized light; D, counterpart, low angle light; E, part, low angle light; F, ROMIP 61669, partial remains of head with sclerotized elements preserved, direct light; G-H, ROMIP 61668, low angle light; G, overview of head; H, closeup showing continuous connection of the P-element necks after dissection through the overlying appendage. A-F, bars=20mm; G-H, bars=10mm. Abbreviations: lm=lamellar band; others as in Figs 1-2.

Page 9 – Supplementary Figure 9: Results of Maximum Parsimony analysis. Strict consensus of 342 MPTs, best score=120 steps. CI=0.510; RI=0.722. Numbers at nodes indicate Bremer decay values | bootstrap percentages.

Page 10 – Supplementary Figure 10: Results of Maximum Likelihood analysis. Majority rule consensus (consensus log likelihood=-631.428). Numbers at nodes indicate ultrafast bootstrap percentages.

Phylogenetic Analysis

Potential synapomorphies for important radiodont clades:

***Cambroraster* + *Zhenghecaris*:**

- Similarities in the shape of the H-element, particularly the broad downcurving lateral areas and posterolateral spinous processes (ch. 3, 29)

Cambroraster + *Zhenghecaris* + ***Hurdia*:**

- Reticulate ornamentation on the carapace elements (ch. 26)
- At least *Cambroraster* and *Hurdia* have a distal section of the frontal appendage with reduced podomeres (ch. 35) and have strongly hooked auxiliary spines (ch. 54) and inner plates in the oral cone (ch. 22)

Cambroraster + *Zhenghecaris* + *Hurdia* + ***Aegirocassis* + *Stanleycaris* + *Pahvantia* + *Peytoia*:**

- Greatly enlarged head carapace complex and posteriorly positioned eyes (ch. 15, 25)
- Posterolateral notches in the H-element (except absent in *Aegirocassis*, questionable in *Peytoia* and *Stanleycaris*; ch. 28)
- P-elements oblong, with irregular outline (except in *Aegirocassis* where they may be subcircular; ch. 30)
- Oral cone with smooth circumoral plates (ch. 21)
- Frontal appendages bearing elongate endites with a strong mesial curvature (ch. 39)

Hurdiidae:

- Absence of a constricted neck region separating the head and trunk (ch. 11)
- Differentiated medial spinous outgrowths on frontal appendage (but lost in some taxa like *Cambroraster*; ch. 38)
- Elongate endites on 5-7 proximal podomeres (ch. 44), lacking posterior auxiliary spines (ch. 48)

Hurdiidae + ***Laminacaris***:

- Pectinate auxiliary spines (ch. 51; potentially convergent with tamisiocaridids) oriented perpendicular to the endite long axis (ch. 52) with an alternation of long and short spines (ch. 53)

Hurdiidae + *Laminacaris* + ***Amplectobelua* + *Lyrarapax***

- Tetraradially arranged plates in oral cone (ch. 20; but questionable for *Laminacaris* and *Amplectobelua*)
- Strong proximodistal differentiation of the appendage (ch. 33)

Tamisiocarididae

- Pair of elongate endites per podomere (ch. 43)
- Endites with 3 or more posterior auxiliary spines (ch. 49)

Radiodonta (excluding *Caryosyntrips*)

- Head carapace complex with central (H-) and lateral (P-) elements (ch. 24)
- Outgrowths from frontal appendages bearing auxiliary spines (ch. 46)
- Reduced anterior flaps or bands of lamellae (ch. 63) and strong tapering of body from anterior to posterior (ch. 65)

Parsimony – Methods

Parsimony optimization was conducted in TNT 1.5 [1]. A heuristic search using New Technology was initiated from a random starting tree and consisted of 1000 replications, each with 5 rounds of the ratchet [2] followed by 5 rounds of tree fusing (xmult: replic 1000 ratchet 5 fuse 5). The search was set to finish if 20 independent hits of the best tree length were encountered (hits 20). Bootstrapping was conducted using 1000 bootstrap replicates, each from 100 replications with 5 rounds of the ratchet (resample boot replic 1000 [xmult = replic 100 ratchet 5]). Bremer support was calculated with tree bisection reconnection, retaining trees suboptimal by 8 steps.

Maximum Likelihood – Methods

Following model selection, maximum likelihood phylogenetic analysis was conducted in IQ-Tree ([3]; -m testmerge -mset MK). The heuristic search was initiated from 1000 starting parsimony trees (-ninit 1000) using the MK+FQ+ASC model and the same partitioning scheme used for Bayesian analysis. Partitions were allowed to evolve at differing rates (-spp; i.e. edge proportional partition model [4]). Nodal support was estimated with 1000 ultrafast bootstrap replicates (-bb) [5].

Lists of Taxa and Characters

The lists of taxa and characters below draw on a number of previous studies, most notably those with a focus on radiodont internal relationships: [6], [7] and its modified versions [8–11]. We have implemented changes to various character definitions and coding and added several new characters (see remarks below each character for details). References to characters in relevant papers are provided where applicable, as well as remarks on our interpretations and coding. References to inferred feeding ecology and functional morphology can also be found below, associated with each taxon.

List of included taxa and references used for their coding:

The following list includes all of the terminal taxa coded in our matrix and the primary references for our coding. Radiodonts are underlined.

Aegirocassis benmoulae Van Roy et al. [9]

Amplectobelua stephenensis Daley & Budd, 2010 [11,12]

Amplectobelua symbrachiata Hou et al. 1995 [13–15]

'Anomalocaris' briggsi Nedin, 1995 [16]*

Anomalocaris canadensis Whiteaves, 1892 [17–21]

Anomalocaris saron Hou et al. 1995 [13,14,22,23]

Aysheaia pedunculata Walcott, 1911 [24]

Cambroraster falcatus Moysiuk & Caron, 2019 (this paper)

Caryosyntrips serratus Daley & Budd, 2010 [12,25]

Chengjiangocaris kunmingensis Yang et al. 2013 [26,27]

Eoredlichia intermediata Lu, 1940 [28]

Habelia optata Walcott, 1912 [29]

Hallucigenia sparsa Walcott, 1911 [30,31]

Hurdia victoria Walcott, 1912 and *Hurdia triangulata* Walcott, 1912 [6,32]**

Isoxys acutangulus Walcott, 1908 & *I. auritus* Jiang, 1982 [33,34]***

Jianshanopodia decora Liu et al. 2006 [35,36]

Kerygmachela kierkegaardi Budd, 1993 [37–39]

Laminacaris chimera Guo et al. 2018 [40]

Lyrarapax unguispinus Cong et al. 2014 & *L. trilobus* Cong et al. 2016 [8,11,41]****

Megadictyon haikouensis Luo and Hu, 1999 [36,42]

Opabinia regalis Walcott, 1912 [43–46]

Ovatiovermis cribratus Aria & Caron, 2017 [47]

Pahvantia hastata Robison & Richards, 1981 [10]

Pambdelurion whittingtoni Budd, 1997 [48–50]

Peytoia nathorsti Walcott, 1911 [9,12,17,21,32]

Ramskoeldia consimilis Cong et al. 2018 [51]

Schinderhannes bartelsi Kuhl et al. 2009 [52]

Siberion lenaicus Dzik, 2011 [53]

Stanleycaris hirpex Pates et al. 2017 [54,55]

Surusicaris elegans Aria & Caron, 2015 [56]

Tamisiocaris borealis Daley & Peel, 2010 [7,57]

Waptia fieldensis Walcott, 1912 [58]

Yawunik kootenayi Aria et al. 2015 [59]

Zhenghecaris shankouensis Vannier et al. 2006 [23]

* This species is highly unlikely to be a member of the genus *Anomalocaris* based on our analysis and previous studies [7,8,10,11].

**Both species were coded with characters pooled under a single terminal as they are differentiated only by the shape of the H-element and would be identical in their coding for all characters in this matrix.

*** Both species were coded with characters pooled under a single terminal to include complementary states that may be unknown in one species.

****Both species were coded with characters pooled under a single terminal as few characters differentiate the putative species and their status as independent species versus morphologically distinct ontogenetic stages has been questioned [11].

Taxa excluded:

We excluded several taxa that have been included in previous analyses, because their incompleteness and poor preservation make them poor candidates for phylogenetic analysis – hurdiid (Fezouata) [60], *Paranomalocaris* [61], *Anomalocaris kunmingensis* [61], *Anomalocaris sp.* (Balang) [62], *Anomalocaris sp. A* (Emu Bay) [16] – or, in the case of *Hurdia sp.* from Utah, because of a lack of evidence for differentiation from species known from the Burgess Shale [63].

General characters

[1] External subdivision of integument, type
0. Annulated
1. Segmented

Remarks: See [7] ch. 12. A segmented integument is present in radiodonts. See in particular *Schinderhannes* [52] and *Aegirocassis* [9], but also *Lyrarapax* [41] in which segmental boundaries are visible crossing the dorsum (their Fig. 1).

[2] Arthrodization of body (tergal sclerites joined by arthrodial membranes)
0. Absent
1. Present

Remarks: See [31] ch. 27; [7] ch. 15. Coded as ? for isoxyids as the presence of arthrodization in these taxa is unclear [56].

[3] Externally developed pleurae
0. Absent
1. Present

Remarks: Modified from [6] ch. 24; [64] ch. 152. We here consider pleurae as lateral or ventrolateral extensions of the tergum which are clearly demarcated from the tergal axis (excluding for example tergo-pleural rings, where the division between the tergum and pleura is indistinct [64]). We code state 1 for *Cambroraster* and *Zhenghecaris* to test whether the enlarged pleura-like lateral areas of the H-element, which project outward from the body and curve down, are optimized as homologous with the pleurae of euarthropods.

[4] Digestive tract with paired diverticulae
0. Absent
1. Present

Remarks: See [6] ch. 16; [7] ch. 16. This character has been proposed as a synapomorphy of euarthropods, radiodonts, and several large lobopodians [36].

[5] Appendicular outgrowths from the body, number per somite

0. Single
1. Paired

Remarks: Modified from [9] ch. 21. This character considers the paired flaps described in *Aegirocassis* [9]. The evidence for paired flaps in *Peytoia* is more equivocal and we code it as ?. In addition, we consider here the typical euarthropod condition, in which the limb is composed of two conjoined rami. This is based on the proposal of Van Roy et al. that the second pair of flaps in *Aegirocassis* are homologous to the outer rami (exites or exopods) of euarthropod biramous limbs. These states are differentiated in the following character. The presence of lobopodous appendages in addition to lateral flaps in *Opabinia*, *Kerygmachela*, and *Pambdelurion* is controversial [38,44–46], and coded as ? here.

[6] Biramous limbs with conjoined endopod and exopod

0. Absent
1. Present

Remarks: See [6] ch. 34; [64] ch. 176. This character is coded as inapplicable for taxa coded as state 0 in the previous character. We provisionally consider the outer limb branches as homologues across the limited sampling of euarthropod taxa included here, acknowledging that the homology of the outer limb branches of fossil euarthropods with either exopods or exites of extant crustaceans remains controversial [65].

[7] One or more pairs of appendages bearing cuticular outgrowths serially arranged along their length

0. Absent
1. Present

Remarks: Modified from [47] ch. 12. We consider the spinous outgrowths on radiodont and euarthropod appendages as well as the softer outgrowths adorning the appendages of many lobopodians (e.g. [38]) in this sovereign character. Terminal claws are not considered here as they are not serially arranged along the length of the appendage. Outgrowths may occur on a single limb pair (as in the frontalmost appendages of e.g. radiodonts) or a series of limbs (e.g. repeated endites on euarthropod limbs); these states are differentiated in character 59. Some taxa also bear a second row of outgrowths, a state considered in character 37.

[8] Arthrodization of one or more pairs of appendages

0. Absent
1. Present

Remarks: See [6] ch. 18; [7] ch. 23. Here we code for a likely developmental homology of radiodonts and euarthropods.

Head characters

[9] Head tagma, defined by the fusion of several anterior tergites and/or differentiation of several pairs of limbs forming a cohesive anteriormost functional unit

0. Absent
1. Present

Remarks: Modified from [47] ch. 6. We code radiodonts as 0. The hurdiid H-element is most likely to be homologous with the interocular sclerite of other radiodonts and some euarthropods (see ch. 23) and we consider the anterior reduced flaps/lamellar bands (see ch. 11) to be insufficiently differentiated to meet the definition of a head tagma.

[10] Tergal sclerotization in head tagma, type

0. Tergites fused together with limited posterior expansion (shield)
1. Cephalic tergites with high degree of posterior expansion, overlapping more posterior segments (carapace)

Remarks: See [64] ch. 34, 35.

[11] Frontalmost head separated from trunk by narrow 'neck' region

0. Absent
1. Present

Remarks: See [66] ch. 35. This character describes the condition in taxa with a head delineated by its frontal position (i.e. not necessarily a head tagma *sensu stricto*). State 1 is characteristic of taxa like *Anomalocaris* [20], and *Lyrarapax* [8,41]. Hurdiids are coded as 0 because their anterior lamellar bands have been subsumed below their greatly enlarged heads, leaving no constriction between head and trunk.

[12] Lateral compound eyes

0. Absent
1. Present

Remarks: Modified from [7] ch. 3. *Kerygmachela* is coded as possessing lateral eyes as interpreted in [39].

[13] Lateral compound eyes, type

0. Sessile
1. Stalked

Remarks: See [6] ch. 11; [7] ch. 4.

[14] Lateral compound eyes, number

0. Two
1. Four or more

Remarks: [New character] Most of the included taxa have a single pair of lateral eyes, but *Yawunik* [59] and *Opabinia* [43] possess a second pair (with the latter also ostensibly bearing a medial eye).

[15] Lateral compound eyes, position

0. Anterior of head, immediately adjacent to the mouth and frontalmost appendages
1. Far posterior to mouth and frontalmost appendages

Remarks: [New character] At least *Cambroraster*, *Peytoia* [17], and most probably *Hurdia* [6,32] are characterized by an extreme posterior dislocation of the eyes, such that they sit posterior to three sets of flaps (see discussion). By inference from the position of the posterolateral notches in the H-element, this is likely to have been the case for most other hurdiids as well, with the notable exception of *Schinderhannes*. In this last taxon, the eyes are positioned anteriorly [52] (state 0), as in taxa like *Lyrarapax* and *Anomalocaris* [8,20].

[16] Mouth, position

0. Anterior
1. Ventral
2. Posterior facing, gut recurved

Remarks: See [7] ch. 6. *Kerygmachela* [39] and *Pambdelurion* [49] are coded as ?, as we think available material remains equivocal as to whether their mouths are positioned ventrally.

[17] Hypostome

0. Absent
1. Present

Remarks: See e.g. [64] ch. 56.

[18] Ring of circumoral sclerites

0. Absent
1. Present

Remarks: See [6] ch. 7; [7] ch. 7. This character does not consider the hypostome-labrum or internal pharyngeal sclerites of euarthropods [67]; such conditions are coded as 0. We consider *Hallucigenia* as state 1 even though it is unclear whether its pharyngeal sclerites form a complete ring and they seem to occur within the buccal cavity instead of strictly surrounding the mouth opening [30]. Whether the oral structures in the large lobopodian taxa [36] are sclerotized is unclear and they have been coded as ?. Likewise, striations surrounding the mouth in *Opabinia* [43] have been interpreted as possible circumoral elements [66], however we code *Opabinia* as ? pending a more detailed evaluation in this taxon. The oral cone of *Lyrarapax* was originally interpreted as lacking sclerotized plates [8]. Based on a recently described specimen, Liu et al. [11] suggested the presence of a sclerotized oral cone, however the preservation of this structure is very poor and we choose to remain ambiguous in our coding for this taxon.

[19] Differentiation of at least two types of sclerites in circumoral ring (i.e. ‘oral cone’)

0. Absent
1. Present

Remarks: See [6] ch. 8; [10] ch. 17.

[20] Circumoral structures, organization

0. Triradial
1. Tetraradial

Remarks: See [7] ch. 9; [10] ch. 18. The oral cones of radiodonts are not strictly radially symmetrical [68], however the arrangement of plates can still be appropriately termed triradial or tetraradial. The oral structure of *Lyrarapax* appears to be tetraradially organized, irrespective of the debate over whether it possessed sclerotized and differentiated plates [8,11]. The hypothetical arrangement of mouth plates in *Amplectobelua symbrachiata* [15] remains too speculative to be coded.

[21] Circumoral plates, ornamentation

0. Smooth
1. Rounded or triangular nodes and furrows

Remarks: See [7] ch. 10. Tentatively coded as state 1 for *Amplectobelua symbrachiata*, despite the fact that the tuberculate plates have never been found as part of the articulated mouth apparatus [15]. The circumoral plates of *A. saron* were reported to be tuberculate [14], but this was not clearly figured, so we have coded this taxon as ?. Pates et al. [63] reported putative nodes in hurdiid material from Utah, however these have never been observed in *Hurdia* and *Peytoia* remains from the Burgess Shale [17,32]; these taxa are coded as state 0 here.

[22] Inner toothed plates in oral cone

0. Absent
1. Present

Remarks: See [6] ch. 9; [7] ch. 11. Present in *Cambroraster* and *Hurdia* [6].

[23] Dorsal interocular sclerite (i.e. anterior sclerite, H-element)

0. Absent
1. Present

Remarks: Modified from [7] ch. 1; see [31] ch. 4. The hurdiid H-element has recently been interpreted as homologous with the interocular (‘anterior’) sclerites of other radiodonts and some euarthropods [10,69], but considering that the former are now recognized to have extended over multiple bands of lamellae, they are reminiscent of the cephalic structures of many euarthropods, in which multiple appendiferous segments are incorporated into a consolidated head tagma [70]. This raises the possibility that the H-element could represent the product of the fusion of several tergites, making it fundamentally different from the small interocular sclerites of other radiodonts. In euarthropods, however, the eyes are either located anterior to or embedded dorsally within the cephalic carapace or shield [71], whereas the eyes of hurdiids reside in an extreme posterior position, behind the H-element (see Discussion). A similar argument might be leveled against the homology of hurdiid head sclerites and isoxyid valves [72], despite other noted similarities in frontal appendage morphology and head structure [56]. In this respect the hurdiid H-element is more comparable in its position with the interocular sclerites of other radiodonts, which always occur near the attachment sites of the pedunculate eyes and the frontal appendages [69]. This homology could be further supported by the presence of a pair of small P-elements adjacent to the interocular sclerites in other radiodonts [8,15]. The

homology of the hurdiid H-element and the interocular sclerite thus seems to be the best-supported hypothesis at present.

[24] Head carapace complex consisting of a dorsal (H-element) and paired lateral or ventrolateral (P-element) sclerites

0. Absent
1. Present

Remarks: See [9] ch. 58. This is most obviously present in hurdiids, which bear highly enlarged H- and P-elements [6]. The narrow necks of the P-elements in these taxa are joined at the front of the head, anterior to the mouth [32]. We also consider the ventrolateral plate-like elements on the head of *Schinderhannes* (originally interpreted as proximal podomeres of the frontal appendage; [52]) to be probable P-elements considering their identical ventrolateral position in comparison with P-elements in e.g. *Peytoia* (see our Fig. 3B,C; also [6]). Further, P-elements ("cowels") were described in *Lyrarapax* [8], with the interocular sclerite forming the central element of the small anterior carapace complex. The state of *Amplectobelua symbrachiata*, recently described as possibly possessing bipartite P-elements [15], is also considered as state 1. Daley & Edgecombe [20] described an interocular sclerite in *Anomalocaris canadensis*, however additional lateral sclerites also appear to be present in their figured material (most notably see their figures 10.2,3 and 11.4,6), which they identified as eyes. We argue that these structures are unlikely to represent eyes as they often occur in partially disarticulated carcases/molts, and their preservation is identical to the interocular sclerite (consistent marginal outline, uniform smooth texture, not reflective in low angle light as would be typical for eyes; see Fig. 3 D, SI Fig. 8). In addition, they bear a strong resemblance to the rounded P-elements in *Amplectobelua*, and occur in an identical position, in close association with the interocular sclerite. In one specimen, the pair of lateral sclerites can even be seen to be connected by a rodiform structure, resembling conjoined P-element necks, as in *Amplectobelua* assemblages (compare our Fig. 3D with [15] Fig. 3) Accordingly, we code *A. canadensis* as state 1 for this character. Non-radiodonts with interocular sclerites but no evidence of associated lateral P-elements (e.g. *Chengjiangocaris*) are coded as state 0 here.

[25] Head carapace complex, size

0. Small, confined to anteriormost area near the claw attachment site, giving the head a trapezoidal shape
1. Large, covering close to half or more of the body length, including several lamellar bands or flaps

Remarks: Modified from [7] ch. 2. In taxa like *Lyrarapax* [8] or *Schinderhannes* (see character above)[52], the carapace complex is a relatively small structure that covers the anterior portion of the head. By contrast, in many hurdiids like *Cambroraster*, *Hurdia*, and *Aegirocassis*, the carapace complex is greatly enlarged, often bearing projecting processes or spines and overlapping several body segments (see discussion). We code *Peytoia* as state 1; although the carapace complex does not project well beyond the margins of the head, the P-elements extend posteriorly beyond at least two bands of lamellae (see Fig. 3B,C). Taxa lacking P-elements but bearing a small interocular sclerite were also coded as state 0.

[26] Head carapace complex, reticulate ornamentation

0. Absent
1. Present

Remarks: [New character] *Hurdia* [32] and *Cambroraster* share conspicuous reticulate ornamentation on their H- and P-elements. Poorly preserved reticulation was also identified in *Zhenghecaris* [23].

[27] Interocular sclerite, anterior margin, shape

0. Pointed or bearing a forward projecting spine
1. Rounded

Remarks: Modified from [9] ch. 59. We do not distinguish between an ogival or spinous anterior margin, as *Hurdia* seems to exhibit morphologies that span a spectrum between these end states (see figured material in [32] and the large variation in shape documented). A detailed quantitative evaluation of hurdiid H-element shape may help to further subdivide this character.

[28] Interocular sclerite with a posteriomedial and pair of posterolateral notches

0. Absent
1. Present

Remarks: See [10] ch. 8. This character is present in many hurdiids, but is exceptionally pronounced in *Cambroraster*, as well as in *Zhenghecaris* ([23] see our SI Fig. 7). In these taxa, the posterolateral notches (accommodating the eyes) separate the axial and lateral areas of the H element posteriorly, while the medial notch results in the bilobation of the posterior margin of the axial area.

[29] Posterolateral tips of interocular sclerite drawn out into elongate processes bearing multiple spines

0. Absent
1. Present

Remarks: [New character] State 1 differentiates *Cambroraster* and *Zhenghecaris* [23], although the spinosity of the former is much greater (SI Fig. 7). By contrast, the H-elements of taxa like *Hurdia* do not extend laterally to the same extent beyond the body and lack spines [6,32]; they are coded as 0.

[30] P-elements, overall shape

0. Subcircular
1. Oblong (length greater than twice width), irregular

Remarks: [New Character] The P-elements of *Hurdia*, *Cambroraster*, and *Peytoia* are much more than twice as long as they are wide, although their ovoid to subrectangular shape is quite variable [6,32]. By contrast, those of *Amplectobelua* [15] and *Anomalocaris* [20], and probably *Aegirocassis* [9] are subcircular. The shape in *Lyrarapax* [8,11] and *Schinderhannes* [52] is unclear owing to poor preservation.

Frontal Appendages

Euarthropods are coded as questionable for most characters in this section in consideration of the debate over the segmental homology of radiodont frontal appendages (for example, see arguments in [8,73]).

Isoxyid frontal appendages are coded as homologous with those of radiodonts considering noted similarities in external morphology [33,56].

A note on the coding of *Pahvantia*: We code characters in the section as questionable for this taxon, as we think that the identity of the structure interpreted as a putative appendage in a single specimen [10] is dubious. The following lines of evidence stand against this structure being interpreted as a radiodont frontal appendage:

- The "endites" of *Pahvantia* show indistinct and wavy margins, consistent with flexibility of these structures; this contrasts with the typical mode of preservation of radiodont endites, which tend to be robustly sclerotized compared to other body parts (see for example discussion in [9] SI)

- The "podomeres" show no differentiation from the "endites" (in fact "auxiliary setae" seem to cross over them as seen in [10] Fig. 1e); they also have wavy, indistinct margins, showing no evidence of sclerotization, podomere boundaries, or arthrodial membranes

- The "peduncle" is extremely narrow, whereas it is usually the broadest part of the radiodont frontal appendage

- *Pahvantia*'s "appendage" is nearly the size of its H-element, far larger in relative size than appendages of other hurdiids (see our Fig. 1g for comparison; the appendages are less than a third the length of the H-element)

The gross morphology of the "appendage" of *Pahvantia* as described above may be more consistent with it representing several bands of lamellae (compare to figured material in [6]). The two putative proximal endites are a possible exception, as their morphology and preservation is more similar to the endites of other hurdiids (compare to material in [32]; this paper fig. 3) and their putative connection to the lamellate structures is unclear. These could possibly represent disarticulated endites partially overlapping the other body elements. Until additional better-preserved specimens can be found, we consider *Pahvantia*'s appendage morphology uncertain.

[31] Strong differentiation of frontalmost pair of appendages from more posterior pairs

0. Absent
1. Present

Remarks: See [47] ch. 5. Euarthropods possess state 1 regardless of whether the labrum is considered the anteriormost appendage pair. Some lobopodians like *Ovatiovermis* [47] and *Hallucigenia* [30] have several anterior differentiated pairs of appendages which are relatively homonomous, a state considered here as 0.

[32] Bases of frontalmost appendages occupying the entire "head," leaving no interspace with trunk appendages

0. Absent
1. Present

Remarks: See [47] ch. 7.

[33] Strong proximodistal differentiation of podomeres and/or endites along appendage

0. Absent
1. Present

Remarks: [New character] Some radiodonts like *Anomalocaris* possess only a single series of essentially homonomous podomeres [21] while others like *Hurdia* and *Amplectobelua* have a frontal appendage with differentiated distal and proximal sections [6,13]. Podomeres of the peduncle and the differentiation of outer spines along the appendage are accounted for in separate characters and are not considered here.

[34] Podomeres in distal articulated portion of arthrodized frontal appendage (including distal tip, but not the peduncle), number

0. 12 or fewer
1. 13 or more

Remarks: Modified from [7] ch. 24. We exclude the proximal peduncular podomeres from our count due to their highly variable expression / preservation (following [10]).

[35] Highly reduced distalmost podomeres

0. Absent
1. Present

Remarks: [New character] State 0, in e.g. *Peytoia,* is defined by no significant change in the diameter of adjacent podomeres along the appendage [32]. By contrast, in *Cambroraster* and *Hurdia* [32], the distalmost section of the frontal appendage is highly reduced in diameter compared to the proximal section (state 1). The reduction in diameter results in a prominent inward flexure between proximal and distal sections. The number of distal podomeres is also reduced compared to e.g. *Peytoia*.

[36] Outward kink separating proximalmost (peduncle, or shaft) and distal portions of the appendage

0. Absent
1. Present

Remarks: See [7] ch. 27.

[37] Pair of spiniform cuticular outgrowths per podomere

0. Absent
1. Present

Remarks: [New character] Most radiodonts have a pair of outgrowths (two endites or endite+medial spinous outgrowth) per frontal appendage podomere [7,21]. Cases where most podomeres bear paired endites, but a proximal podomere bears a hypertrophied unpaired endite (e.g. *Amplectobelua symbrachiata;* [13]) are considered in a subsequent character and are coded as state 1 here. *Cambroraster, Hurdia,* and *Aegirocassis* seem to lack a second set of outgrowths. *Caryosyntrips camurus* was interpreted to possibly possess a pair of endites per podomere [25]; we code *Caryosyntrips serratus* as ? here. It should be noted that most radiodonts also possess a third set of spines along their appendage outer surface (often called dorsal spines, or here outer spines), which are considered in character 55.

[38] Pair of spiniform cuticular outgrowths per podomere, type

0. Both outgrowths similar and located on the inside of appendage (second endite)

1. Outgrowths morphologically differentiated, one located on the inside (endite) and one on the medial side of appendage (medial spinous outgrowth)

Remarks: Modified from [7] ch. 45. Spiniform outgrowths occurring on the inside of the radiodont appendage are commonly termed endites, by positional comparison with structures on euarthropod limbs. We employ the term medial spinous outgrowth here to describe cuticular projections bearing multiple spines, pointing toward the midline of the animal. These are characteristically found in some hurdiids. In addition to their differing location, medial spinous outgrowths are morphofunctionally differentiated from endites on the same podomere. Medial spinous outgrowths are notably well-developed in *Peytoia* [12,21,32] and *Stanleycaris* [54].

[39] Endites, curvature

0. Straight
1. Curving mesially around the mouth, forming a basket

Remarks: [New character] Vinther et al. ([7] ch. 39, 46; also [9,32]) interpreted the endites of some hurdiids as hooked anterodorsally at their tips, and with proximal endites curved gently posteriorly. Pates et al. [63] considered the varying flexure of the endites a taphonomic artefact due to deformation of originally straight endites. We agree with Pates et al. that the variation in curvature between specimens is taphonomic in origin, but based on well-preserved *Cambroraster* material (corroborated by observation of appendages of *Hurdia*, *Peytoia*, *Stanleycaris* (see our Fig. 3), and figured material of other hurdiids; [12,21,32,54]), we argue that the endites of these taxa were originally mesially curved (see Discussion). When compressed in perfect lateral view the endites appear straight (although the distal ends are deformed by compression or project into the matrix; e.g. Figs 2A, 3H), but in oblique view they may appear to bend forward or backward to varying degrees, depending on the exact angle of burial. In frontal view the mesial curvature is most evident (e.g. Figs 2C, 3G). We have coded taxa like *Kerygmachela*, with seemingly less-sclerotized appendicular outgrowths as ?.

[40] Endites, attachment angle

0. Projecting straight from the supporting podomere
1. Projecting forward at an acute angle to the distal end of the appendage

Remarks: See [7] ch. 35.

[41] Adjacent endites, alternation in relative length

0. Absent
1. Present

Remarks: See [7] ch. 44.

[42] One or more endites elongate (at least 1.5 times the height of the supporting podomere)

0. Absent
1. Present

Remarks: This character is similar to that introduced in [7] (ch. 31), except that they chose to exclude cases of a single elongate endite, with the intention of distinguishing between the typical state for hurdiids (multiple elongate endites) and amplectobeluids

(single hypertrophied endite). We make this distinction in character 44, but we choose not to exclude the potential homology of this type of endite morphology across both groups, considering in particular the recently published appendages of *Laminacaris* which show a blend of morphologies seen in both groups [40].

[43] Elongate endites, number per podomere

0. Single
1. Paired

Remarks: [New character] In some taxa like the hurdiids, *Lyrarapax*, and *Amplectobelua symbrachiata*, only a single elongate endite is present per podomere [6,8,13,21]. In *'Anomalocaris' briggsi, Tamisiocaris*, and *Amplectobelua stephenensis* there are a pair of similar elongate endites on one or more podomeres [7,12,16].

[44] Elongate endites, location

0. Hypertrophied endite(s) on one or two proximal podomeres opposing the appendage tip to form a claw
1. Elongate endites on 5-7 proximal podomeres

Remarks: Modified from [7] ch. 31, 36. States 0 and 1 differentiate amplectobeluids and hurdiids. We have coded *Laminacaris* as state 0 to emphasize the similarity with the state in amplectobeluids, although unlike these taxa it also appears to have a second proximal elongate endite (poorly preserved in figured material; [40]). *'Anomalocaris' briggsi* and *Tamisiocaris* are coded as inapplicable, as the combination of elongate and homonomous endites in these taxa [7,16] renders this character redundant for them.

[45] Multiple elongate endites, relative length

0. Subequal along appendage
1. Size decreases distally

Remarks: [New character] Exemplified by the difference between *Hurdia* ([6]; see Fig. 3D; state 1) and *Cambroraster* (see Fig. 2A; state 0).

[46] One or more appendicular outgrowths (endite or medial spinous outgrowth) bearing auxiliary spines

0. Absent
1. Present

Remarks: See [7] ch. 37. This is shared by most radiodonts, with the notable exception of *Caryosyntrips* [12,25].

[47] Auxiliary spines, serial occurrence

0. Present on only one endite
1. Present on multiple endites

Remarks: See [10] ch. 37. *Lyrarapax* appears to have multiple endites bearing auxiliary spines [8,41] and is coded as 1 despite otherwise poor preservation of the endites in published material.

[48] Posterior auxiliary spines on endites

0. Absent

1. Present

Remarks: See [7] ch. 42. Coded as 1 if posterior auxiliary spines are present on any endite.

[49] Posterior auxiliary spines, maximum number per endite

0. One or two
1. Three or more

Remarks: Modified from [7] ch. 43. State 1 differentiates *Tamisiocaris* and '*Anomalocaris' briggsi*. We code for the maximum number rather than the modal number under the assumption that loss of a structure is more probable than its gain, therefore maximum number may carry more phylogenetic signal.

[50] Anterior auxiliary spines, maximum number per endite

0. 1
1. 2-5
2. 6-10
3. 11 or more

Remarks: Modified from [7] ch. 40. Although the 'setae' of *Aegirocassis* clearly differ in structuro-functionally important ways from the auxiliary 'spines' of other hurdiids [9], we disagree with the decision to consider them as non-homologous [10]. Setae and spines are impossible to conclusively differentiate without ultrastructural data, and when this is unavailable, the equivalent position of cuticular projections in closely related taxa has been suggested to be justifiable grounds for hypothesizing homology ([74], p. 171). The condition in *Cambroraster*, which has elongate auxiliary spines in similar number and identical position to the setae of *Aegirocassis*, provides a plausible link with other hurdiids. We have coded other characters relating to auxiliary 'spines' accordingly for *Aegirocassis*.

[51] Auxiliary spines on endites, arrangement of multiple spines

0. Radiating from base of endite
1. Pectinate (arranged in parallel along the endite)

Remarks: See Vinther et al. 2014 ch. 38. *Lyrarapax* was originally described as possessing pectinate arrangement on its hypertrophied proximal endite [8], but we think it is more appropriately described as radiating, given that all spines emerge from a point at the base of the endite and distal spines are nearly parallel to the endite axis while proximal spines protrude at a much steeper angle. In '*Anomalocaris' briggsi*, spines radiate from the base of the endite, while distally the spines are arranged in pectinate fashion [16]; it is accordingly coded as polymorphic.

[52] Auxiliary spines on endites, angle

0. Directed distally, at an acute angle to the tip of the endite
1. Directed roughly perpendicular to the endite long axis

Remarks: See [7] ch. 41.

[53] Alternation of long and short auxiliary spines on pectinate endite

0. Present

1. Absent

Remarks: [New character] Guo et al. [40] recently noted this character as potentially phylogenetically significant. In at least *Cambroraster*, *Hurdia*, *Peytoia* (see figs. in [12,21,32]), and *Laminacaris* [40], there is a conspicuous alternation of long and short auxiliary spines along the length of the pectinate endites.

[54] Auxiliary spines, curvature

0. Straight
1. Strongly hooked

Remarks: [New character] *Cambroraster* and *Hurdia*, are unique in possessing strongly hooked auxiliary spines (see discussion). Coded as inapplicable for *Aegirocassis*.

[55] Outer spines

0. Absent or highly reduced
1. Present

Remarks: See [7] ch. 30. These structures have been referred to simply as "dorsal" spines, although we prefer the description "outer" for this surface of the appendage [56]. These are independent of the medial spinous outgrowths / second set of endites, as both can co-occur on a single podomere (e.g. consider *Peytoia* or *Anomalocaris*; [21]). They are arranged in a row along the outside of the appendage in most radiodont taxa, and usually increase in size distally. In some hurdiids like *Cambroraster*, they are absent (except for possibly the tiny reduced spines on podomeres eight and nine). We also code these structures as present in *Surusicaris* [56].

[56] Distalmost outer spines, type

0. Weakly curving and finely tapering
1. Strongly recurved (talon-like) and robust

Remarks: [New character] This character differentiates the state (1) in *Amplectobelua* and *Peytoia* (see discussion in [12,32]) from that in other radiodonts.

Trunk characters

[57] Sternites

0. Absent
1. Present

Remarks: See [64] ch. 54.

[58] Arthrodization of post-frontal appendages

0. Absent
1. Present

Remarks: See [47] ch. 34. Coded as state 0 for all radiodonts.

[59] Post-frontal appendages bearing serially arranged cuticular outgrowths

0. Absent

1. Present

Remarks: Modified from [47] ch. 46. We consider segmentally repeated endites / exites present in many euarthropods as state 1, as well as the softer outgrowths on the limbs of some lobopodians (e.g. *Aysheaia;* [24]). This is consistent with our coding of probable serially homologous structures on the frontal appendages of euarthropods, radiodonts, and lobopodians in character 7. *Siberion* [53] was reconstructed as bearing fleshy outgrowths on its trunk appendages, but this is not visible in the figured material. Radiodonts and *Opabinia* are coded as state 0 here, as lamellae are considered in character 67.

[60] Gnathobases

0. Absent
1. Present

Remarks: See [64] ch. 174. Coded as ? in *Amplectobelua* and *Ramskoeldia*. The homology of "gnathobase-like structures" recently described in these taxa and the gnathobases of euarthropods remains equivocal [15,51].

[61] Lobopodous appendages, shape

0. Equal to or shorter than body diameter, conical
1. Elongate, significantly longer than body width, cylindrical

Remarks: See [47] ch. 32.

[62] Trunk appendages are lateral flaps

0. Absent
1. Present

Remarks: See [6] ch. 36; [9] ch. 49.

[63] Reduced anterior flaps or bands of lamellae

0. Absent
1. Present

Remarks: See [66] ch. 71. Many radiodonts have 3 or possibly 4 reduced flaps on a narrow neck region [8,11,14,20,41]. Hurdiids like *Cambroraster* also seem to bear corresponding reduced anterior lamellar bands, although it is unknown if these are associated with flaps [17,32]. By contrast, taxa like *Opabinia* [45] and *Kerygmachela* [39] lack such anterior differentiation of flaps.

[64] Main trunk flaps, number

0. 8-9
1. 10-12
2. 13 or more

Remarks: Modified from [7] ch. 19. Ranges in the numbers for each state vary to accommodate some uncertainty due to imperfect specimen preservation. We define "main" trunk flaps to exclude the reduced anterior flaps and tail fan blades (which have been hypothesized to be derived from modified flaps; [7]). We have tentatively coded *A. saron* for state 1 based on [14]. A well-preserved juvenile of *Lyrarapax unguispinus* was recently described [11] showing probably eight main flap pairs,

however considering the small size of this individual, the adult number of flaps could have been greater. Incomplete specimens of *Lyrarapax trilobus* suggest at least 10 pairs of flaps [41]; it is unclear whether this species is synonymous with *L. unguispinus* as pointed out by Liu et al. [11]. We therefore remain ambiguous in our coding for this taxon.

[65] Relative width of trunk at anterior and posterior segments

0. Body less than three times as wide at the anterior as at the posterior
1. Body at least three times as wide at the anterior as at the posterior

Remarks: See [7] ch. 13. This character distinguishes between the state in at least *Kerygmachela* and *Opabinia*, which have subcylindrical bodies (0) and that of radiodonts which typically have more triangular trunk shape (1). This character considers only the portion of the trunk bearing main body flaps and does not account for the reduced anterior 'neck' present in some radiodonts, which is coded in character 11.

[66] Flap rays

0. Absent
1. Present

Remarks: See [7] ch. 52. Linear structures have long been documented within the lateral flaps of radiodonts (often called rays, veins, transverse lines, or strengthening rays). In *Peytoia* [9,17] these structures run parallel to the proximo-distal axis of the flap and occur throughout, from anterior to posterior. A similar situation appears to be the case for *Aegirocassis*, although the cone-in-cone structure of these 'rays' has yet to be identified in other radiodonts [9]. In *Anomalocaris saron* [14], *Lyrarapax* [11,41], *Ramskoeldia* [51], and *Amplectobelua symbrachiata* [14,15], the ray structure appears different. The flap is divided by a longitudinal line into an anterior zone with rays, which appears thicker and better preserved, and a posterior zone lacking any evidence of rays. In the anterior zone the widely dispersed rays are directed on a diagonal in an anterodistal direction. A similar morphology is found in isolated flaps from Emu Bay [16]. Despite the possible differences between taxa, we provisionally code all rays as potentially homologous until a more detailed evaluation of this character has been conducted. *Anomalocaris canadensis* has very fine surficial striations running anterior to posterior on the flaps, a situation that seems to be unlike other taxa [20], justifying our coding as state 0. We code *Cambroraster* and *Hurdia* [32], as ? here.

[67] Lamellae

0. Absent
1. Present

Remarks: See [6] ch. 41; [7] ch. 50. We tentatively code the bands of lamellae ('setal blades') in radiodonts as homologous with euarthropod lamellae [6]. Suzuki & Bergström [75] have argued that 'proximal lamellae' in xiphosurans are non-homologous to the exopodial lamellae of artiopodans, citing structural and topological differences. Considering the limited sampling of euarthropod taxa in this matrix, we do not distinguish between proximal and exopodial lamellae here, but we recognize that this putative homology remains to be fully tested.

[68] Lamellae, position

0. Arranged in bands crossing the body and appendages
1. On appendages only

Remarks: See [7] ch. 51. In euarthropods like trilobites, lamellae tend to be positioned exclusively on the exopods, although proximal lamellae may extend slightly onto the body in xiphosurans [75]. By contrast, in at least some radiodonts, lamellae extend over the body in a transverse band from the flaps nearly to the midline. In *Peytoia* [6,17] the lamellae are connected to crenulated attachment structures spanning the body of the animal. Our coding reflects the difference in position of lamellae in taxa like *Peytoia* versus in euarthropods, although the state is less clear in other radiodonts (e.g. *Anomalocaris canadensis* [20]).

[69] Differentiated posterior blades

0. Absent
1. Present

Remarks: See [6] ch. 42; [7] ch. 53. We include the tail fans and furcae of radiodonts, isoxyids, and *Opabinia* under this sovereign character. We differentiate between types of differentiation below, as tail fans and furcae may occur independently (e.g. only furcae in *Lyrarapax* [11]). *Jianshanopodia* has been interpreted to bear a tail fan [35], but the bloated tripartite structure seen in a single poorly preserved specimen does not appear comparable to the bona fide tail fans of radiodonts, so we have coded it as ?.

[70] Tail fan, type

0. Single pair of lobes
1. Several pairs of lobes

Remarks: See [9] ch. 55. Tail fan morphology appears to be quite variable among radiodonts, although in most taxa it is poorly preserved. *Hurdia* [32] and *Schinderhannes* [52] bear only a single pair of blades, whereas *Anomalocaris canadensis* bears three [20], *A. saron* bears two plus furcae [14], and *Cambroraster* likely bears two.

[71] Caudal furcae

0. Absent
1. Present

Remarks: See [7] ch. 54. We code furcae as present in *Lyrarapax*, following [11].

[72] Telson

0. Absent
1. Present

Remarks: See [64] ch. 201. The posterior terminal spine of *Schinderhannes* [52] and *Kerygmachela* [39] resembles the telson of euarthropods, and we code them as state 1 to see if they can be optimized as homologous.

Supplementary References

1. Goloboff PA, Farris JS, Nixon KC. 2008 TNT, a free program for phylogenetic analysis. *Cladistics* **24**, 774–786. (doi:10.1111/j.1096-0031.2008.00217.x)

2. Nixon KC. 1999 The parsimony ratchet, a new method for rapid parsimony analysis. *Cladistics* **15**, 407–414. (doi:10.1006/clad.1999.0121)

3. Nguyen LT, Schmidt HA, Von Haeseler A, Minh BQ. 2015 IQ-TREE: A fast and effective stochastic algorithm for estimating maximum-likelihood phylogenies. *Mol. Biol. Evol.* **32**, 268–274. (doi:10.1093/molbev/msu300)

4. Chernomor O, Von Haeseler A, Minh BQ. 2016 Terrace Aware Data Structure for Phylogenomic Inference from Supermatrices. *Syst. Biol.* **65**, 997–1008. (doi:10.1093/sysbio/syw037)

5. Minh BQ, Nguyen MAT, Von Haeseler A. 2013 Ultrafast approximation for phylogenetic bootstrap. *Mol. Biol. Evol.* **30**, 1188–1195. (doi:10.1093/molbev/mst024)

6. Daley AC, Budd GE, Caron JB, Edgecombe GD, Collins D. 2009 The Burgess Shale anomalocaridid *Hurdia* and its significance for early euarthropod evolution. *Science (80-.).* **323**, 1597–1600. (doi:10.1126/science.1169514)

7. Vinther J, Stein M, Longrich NR, Harper DAT. 2014 A suspension-feeding anomalocarid from the Early Cambrian. *Nature* **507**, 496. (doi:10.1038/nature13010)

8. Cong P, Ma X, Hou X, Edgecombe GD, Strausfeld NJ. 2014 Brain structure resolves the segmental affinity of anomalocaridid appendages. *Nature* **513**, 538. (doi:10.1038/nature13486)

9. Van Roy P, Daley AC, Briggs DEG. 2015 Anomalocaridid trunk limb homology revealed by a giant filter-feeder with paired flaps. *Nature* **522**, 77. (doi:10.1038/nature14256)

10. Lerosey-Aubril R, Pates S. 2018 New suspension-feeding radiodont suggests evolution of microplanktivory in Cambrian macronekton. *Nat. Commun.* **9**, 3774. (doi:10.1038/s41467-018-06229-7)

11. Liu J, Lerosey-Aubril R, Steiner M, Dunlop JA, Degan S, Paterson JR. 2018 Origin of raptorial feeding in juvenile euarthropods revealed by a Cambrian radiodontan. *Natl. Sci. Rev.* **5**, 863–869.

12. Daley AC, Budd GE. 2010 New anomalocaridid appendages from the Burgess Shale, Canada. *Palaeontology* **53**, 721–738. (doi:10.1111/j.1475-4983.2010.00955.x)

13. Xian-Guang H, Bergström J, Ahlberg P. 1995 *Anomalocaris* and other large animals in the Lower Cambrian Chengjiang fauna of southwest China. *GFF* **117**, 163–183. (doi:10.1080/11035899509546213)

14. Chen JY, Ramsköld L, Zhou GQ. 1994 Evidence for monophyly and arthropod affinity of Cambrian giant predators. *Science (80-.).* **264**, 1304–1308. (doi:10.1126/science.264.5163.1304)

15. Cong P, Daley AC, Edgecombe GD, Hou X. 2017 The functional head of the Cambrian radiodontan (stem-group Euarthropoda) *Amplectobelua symbrachiata*. *BMC Evol. Biol.* **17**, 208. (doi:10.1186/s12862-017-1049-1)

16. Daley AC, Paterson JR, Edgecombe GD, García-Bellido DC, Jago JB. 2013 New anatomical information on *Anomalocaris* from the Cambrian Emu Bay Shale of South Australia and a reassessment of its inferred predatory habits. *Palaeontology* **56**, 971–990. (doi:10.1111/pala.12029)

17. Whittington HB, Briggs DEG. 1985 The Largest Cambrian Animal, *Anomalocaris*, Burgess Shale, British Columbia. *Philos. Trans. R. Soc. B Biol. Sci.* **309**, 569–609. (doi:10.1098/rstb.1985.0096)

18. Collins D. 1996 The 'evolution' of *Anomalocaris* and its classification in the arthropod class Dinocarida (nov.) and order Radiodonta (nov.). *J. Paleontol.* **70**, 280–293. (doi:10.1017/S0022336000023362)

19. Daley AC, Bergström J. 2012 The oral cone of *Anomalocaris* is not a classic 'peytoia'. *Naturwissenschaften* **99**, 501–504. (doi:10.1007/s00114-012-0910-8)

20. Daley AC, Edgecombe GD. 2014 Morphology of *Anomalocaris canadensis* from the Burgess Shale. *J. Paleontol.* **88**, 68–91. (doi:10.1666/13-067)

21. Briggs DEG. 1979 *Anomalocaris*: The largest known Cambrian arthropod. *Palaeontology* **22**, 631–664.

22. Vannier J. 2009 The Cambrian explosion and the emergence of modern ecosystems. *Comptes Rendus Palevol* **8**, 133–154. (doi:10.1016/j.crpv.2008.10.006)

23. Zeng H, Zhao F, Yin Z, Zhu M. 2018 Morphology of diverse radiodontan head sclerites from the early Cambrian Chengjiang Lagerstätte, south-west China. *J. Syst. Palaeontol.* **16**, 1–37. (doi:10.1080/14772019.2016.1263685)

24. Whittington HB. 1978 The Lobopod Animal *Aysheaia pedunculata* Walcott, Middle Cambrian, Burgess Shale, British Columbia. *Philos. Trans. R. Soc. B Biol. Sci.* **284**, 165–197. (doi:10.1098/rstb.1979.0010)

25. Pates S, Daley AC. 2017 *Caryosyntrips*: a radiodontan from the Cambrian of Spain, USA and Canada. *Pap. Palaeontol.* **3**, 461–470. (doi:10.1002/spp2.1084)

26. Yang J, Ortega-Hernández J, Legg DA, Lan T, Hou JB, Zhang XG. 2018 Early Cambrian fuxianhuiids from China reveal origin of the gnathobasic protopodite in euarthropods. *Nat. Commun.* **9**, 470. (doi:10.1038/s41467-017-02754-z)

27. Yang J, Ortega-Hernández J, Butterfield NJ, Zhang XG. 2013 Specialized appendages in fuxianhuiids and the head organization of early euarthropods. *Nature* **494**, 468. (doi:10.1038/nature11874)

28. Hou X, Clarkson ENK, Yang J, Zhang X, Wu G, Yuan Z. 2008 Appendages of early Cambrian *Eoredlichia* (Trilobita) from the Chengjiang biota, Yunnan, China. *Earth Environ. Sci. Trans. R. Soc. Edinburgh* **99**, 213–223. (doi:10.1017/S1755691009008093)

29. Aria C, Caron JB. 2017 Mandibulate convergence in an armoured Cambrian stem chelicerate. *BMC Evol. Biol.* **17**, 261. (doi:10.1186/s12862-017-1088-7)

30. Smith MR, Caron JB. 2015 *Hallucigenia*'s head and the pharyngeal armature of early ecdysozoans. *Nature* **523**, 75. (doi:10.1038/nature14573)

31. Smith MR, Ortega-Hernández J. 2014 *Hallucigenia*'s onychophoran-like claws and the case for Tactopoda. *Nature* **514**, 363. (doi:10.1038/nature13576)

32. Daley AC, Budd GE, Caron JB. 2013 Morphology and systematics of the anomalocaridid arthropod *Hurdia* from the Middle Cambrian of British Columbia and Utah. *J. Syst. Palaeontol.* **11**, 743–787. (doi:10.1080/14772019.2012.732723)

33. Legg DA, Vannier J. 2013 The affinities of the cosmopolitan arthropod *Isoxys* and its implications for the origin of arthropods. *Lethaia* **46**, 540–550. (doi:10.1111/let.12032)

34. Vannier J, García-Bellido DC, Hu SX, Chen AL. 2009 Arthropod visual predators in the early pelagic ecosystem: Evidence from the Burgess Shale and Chengjiang biotas. *Proc. R. Soc. B Biol. Sci.* **276**, 2567–2574. (doi:10.1098/rspb.2009.0361)

35. Liu J, Shu D, Han J, Zhang Z, Zhang X. 2006 A large xenusiid lobopod with complex appendages from the Lower Cambrian Chengjiang Lagerstätte. *Lethaia* **51**, 215–222.

36. Vannier J, Liu J, Lerosey-Aubril R, Vinther J, Daley AC. 2014 Sophisticated digestive systems in early arthropods. *Nat. Commun.* **5**, 3641. (doi:10.1038/ncomms4641)

37. Budd G. 1993 A Cambrian gilled lobopod from Greenland. *Nature* **364**, 709. (doi:10.1038/364709a0)

38. Budd GE. 1998 The morphology and phylogenetic significance of *Kerygmachela kierkegaardi* Budd (Buen Formation, Lower Cambrian, N Greenland). *Trans. R. Soc. Edinb. Earth Sci.* **89**, 249–290. (doi:10.1017/S0263593300002418)

39. Park TYS *et al.* 2018 Brain and eyes of *Kerygmachela* reveal protocerebral ancestry of the panarthropod head. *Nat. Commun.* **9**, 1019. (doi:10.1038/s41467-018-03464-w)

40. Guo J, Pates S, Cong P, Daley AC, Edgecombe GD, Chen T, Hou X. 2018 A new radiodont (stem Euarthropoda) frontal appendage with a mosaic of characters from the Cambrian (Series 2 Stage 3) Chengjiang biota. *Pap. Palaeontol.* **5**, 99–110. (doi:10.1002/spp2.1231)

41. Cong P, Daley AC, Edgecombe GD, Hou X, Chen A. 2016 Morphology of the Radiodontan *Lyrarapax* from the Early Cambrian Chengjiang Biota. *J. Paleontol.* **90**, 663–671. (doi:10.1017/jpa.2016.67)

42. Liu J, Shu D, Han J, Zhang Z, Zhang X. 2007 Morpho-anatomy of the lobopod *Magadictyon cf. haikouensis* from the Early Cambrian Chengjiang Lagerstätte, South China. *Acta Zool.* **88**, 279–288. (doi:10.1111/j.1463-6395.2007.00281.x)

43. Whittington HB. 1975 The Enigmatic Animal *Opabinia regalis*, Middle Cambrian, Burgess Shale, British Columbia. *Philos. Trans. R. Soc. B Biol. Sci.* **271**, 1–43. (doi:10.1098/rstb.1975.0033)

44. Budd GE. 1996 The morphology of *Opabinia regalis* and the reconstruction of the arthropod stem-group. *Lethaia* **29**, 1–14. (doi:10.1111/j.1502-3931.1996.tb01831.x)

45. Budd GE, Daley AC. 2012 The lobes and lobopods of *Opabinia regalis* from the middle Cambrian Burgess Shale. *Lethaia* **45**, 83–95. (doi:10.1111/j.1502-3931.2011.00264.x)

46. Zhang X, Briggs DEG. 2007 The nature and significance of the appendages of *Opabinia* from the Middle Cambrian Burgess Shale. *Lethaia* **40**, 161–173. (doi:10.1111/j.1502-3931.2007.00013.x)

47. Caron JB, Aria C. 2017 Cambrian suspension-feeding lobopodians and the early radiation of panarthropods. *BMC Evol. Biol.* **17**, 29. (doi:10.1186/s12862-016-0858-y)

48. Budd GE. 1997 Stem group arthropods from the Lower Cambrian Sirius Passet fauna of North Greenland. In *Arthropod Relationships*, pp. 125–138. Dordrecht: Springer. (doi:10.1007/978-94-011-4904-4_11)

49. Vinther J, Porras L, Young FJ, Budd GE, Edgecombe GD. 2016 The mouth apparatus of the Cambrian gilled lobopodian *Pambdelurion whittingtoni*. *Palaeontology* **59**, 841–849. (doi:10.1111/pala.12256)

50. Young FJ, Vinther J. 2017 Onychophoran-like myoanatomy of the Cambrian gilled lobopodian *Pambdelurion whittingtoni*. *Palaeontology* **60**, 27–54. (doi:10.1111/pala.12269)

51. Cong PY, Edgecombe GD, Daley AC, Guo J, Pates S, Hou XG. 2018 New radiodonts with gnathobase-like structures from the Cambrian Chengjiang biota and implications for the systematics of Radiodonta. *Pap. Palaeontol.* **4**, 605–621. (doi:10.1002/spp2.1219)

52. Kühl G, Briggs DEG, Rust J. 2009 A great-appendage arthropod with a radial mouth from the Lower Devonian Hunsrück Slate, Germany. *Science (80-.).* **323**, 771–773. (doi:10.1126/science.1166586)

53. Dzik J. 2011 The xenusian-to-anomalocaridid transition within the lobopodians. *Boll. della Soc. Paleontol. Ital.* **50**, 65–74.

54. Caron JB, Gaines RR, Mángano MG, Streng M, Daley AC. 2010 A new Burgess Shale-type assemblage from the 'thin' Stephen Formation of the southern Canadian Rockies. *Geology* **38**, 811–814. (doi:10.1130/G31080.1)

55. Pates S, Daley AC, Ortega-Hernández J. 2017 *Aysheaia prolata* from the Utah Wheeler Formation (Drumian, Cambrian) is a frontal appendage of the radiodontan *Stanleycaris*. *Acta Palaeontol. Pol.* **62**, 619–625.

56. Aria C, Caron JB. 2015 Cephalic and limb anatomy of a new isoxyid from the Burgess Shale and the role of 'stem bivalved arthropods' in the disparity of the frontalmost appendage. *PLoS One* **10**, e0124979. (doi:10.1371/journal.pone.0124979)

57. Daley AC, Peel JS. 2010 A possible anomalocaridid from the Cambrian Sirius Passet Lagerstätte, North Greenland. *J. Paleontol.* **84**, 352–355. (doi:10.1007/BF01833437)

58. Vannier J, Aria C, Taylor RS, Caron JB. 2018 *Waptia fieldensis* Walcott, a mandibulate arthropod from the middle Cambrian Burgess Shale. *R. Soc. Open Sci.* **5**, 172206. (doi:10.1098/rsos.172206)

59. Aria C, Caron JB, Gaines R. 2015 A large new leanchoiliid from the Burgess Shale and the influence of inapplicable states on stem arthropod phylogeny. *Palaeontology* **58**, 629–660. (doi:10.1111/pala.12161)

60. Van Roy P, Briggs DEG. 2011 A giant Ordovician anomalocaridid. *Nature* **473**, 510. (doi:10.1038/nature09920)

61. Wang YY, Huang DY, Hu SX. 2013 New anomalocardid frontal appendages from the Guanshan biota, eastern Yunnan. *Chinese Sci. Bull.* **58**, 3937–3942. (doi:10.1007/s11434-013-5908-x)

62. Liu Q. 2013 The first discovery of anomalocaridid appendages from the Balang Formation (Cambrian Series 2) in Hunan, China. *Alcheringa* **37**, 338–343. (doi:10.1080/03115518.2013.753767)

63. Pates S, Daley AC, Lieberman BS. 2018 Hurdiid radiodontans from the middle Cambrian (Series 3) of Utah. *J. Paleontol.* **92**, 99–113. (doi:10.1017/jpa.2017.11)

64. Aria C, Caron JB. 2017 Burgess Shale fossils illustrate the origin of the mandibulate body plan. *Nature* **545**, 89–92. (doi:10.1038/nature22080)

65. Wolff C, Scholtz G. 2008 The clonal composition of biramous and uniramous arthropod limbs. *Proc. R. Soc. B Biol. Sci.* **275**, 1023–1028. (doi:10.1098/rspb.2007.1327)

66. Yang J, Ortega-Hernández J, Gerber S, Butterfield NJ, Hou J, Lan T, Zhang X. 2015 A superarmored lobopodian from the Cambrian of China and early disparity in the evolution of Onychophora. *Proc. Natl. Acad. Sci.* **112**, 8678–8683.

67. Elzinga RJ. 1998 Microspines in the alimentary canal of Arthropoda, Onychophora, Annelida. *Int.*

J. Insect Morphol. Embryol. **27**, 341–349. (doi:10.1016/S0020-7322(98)00027-0)

68. Zeng H, Zhao F, Yin Z, Zhu M. 2018 A new radiodontan oral cone with a unique combination of anatomical features from the early Cambrian Guanshan Lagerstätte, eastern Yunnan, South China. *J. Paleontol.* **92**, 40–48. (doi:10.1017/jpa.2017.77)

69. Ortega-Hernández J. 2015 Homology of Head Sclerites in Burgess Shale Euarthropods. *Curr. Biol.* **25**, 1625–1631. (doi:10.1016/j.cub.2015.04.034)

70. Richter S, Stein M, Frase T, Szucsich NU. 2013 The arthropod head. In *Arthropod Biology and Evolution: Molecules, Development, Morphology* (eds A Minelli, G Fusco, GA Boxshall), pp. 223–240. Verlag Berlin Heidelberg: Springer. (doi:10.1007/978-3-642-36160-9_10)

71. Strausfeld NJ, Ma X, Edgecombe GD, Fortey RA, Land MF, Liu Y, Cong P, Hou X. 2016 Arthropod eyes: The early Cambrian fossil record and divergent evolution of visual systems. *Arthropod Struct. Dev.* **45**, 152–172. (doi:10.1016/j.asd.2015.07.005)

72. Legg DA, Sutton MD, Edgecombe GD, Caron J-B. 2012 Cambrian bivalved arthropod reveals origin of arthrodization. *Proc. R. Soc. B Biol. Sci.* **279**, 4699–4704. (doi:10.1098/rspb.2012.1958)

73. Haug JT, Waloszek D, Maas A, Liu Y, Haug C. 2012 Functional morphology, ontogeny and evolution of mantis shrimp-like predators in the Cambrian. *Palaeontology* **55**, 369–399. (doi:10.1111/j.1475-4983.2011.01124.x)

74. Garm A, Watling L. 2015 The Crustacean Integument: Setae, Setules, and Other Ornamentation. In *Functional Morphology and Diversity* (eds L Watling, M Thiel), Oxford University Press. (doi:10.1093/acprof:osobl/9780195398038.003.0006)

75. Suzuki Y, Bergström J. 2008 Respiration in trilobites: A reevaluation. *GFF* **130**, 211–229. (doi:10.1080/11035890809452774)

Moysiuk & Caron 2019 - Figured Specimens List

Locality	Field # (ROM)	ROMIP	NIGPAS	USNM	Taxon	Figure No.	Type
Marble Canyon	2014-1221	65093			*Cambroraster falcatus*	1 E,F; S3	
Tokumm	2014-0163	65077			*Cambroraster falcatus*	S1 E	
Tokumm	2014-0314	65078			*Cambroraster falcatus*	1 A-D; S2	Holotype
Tokumm	2018-0964	65079			*Cambroraster falcatus*	1 G-I; 2 E; S5 C-D	Paratype
Tokumm	2018-0912	65080			*Cambroraster falcatus*	1 J; 2 C	
Tokumm	2018-0949	65081			*Cambroraster falcatus*	1 K	Paratype
Tokumm	2018-0547	65082			*Cambroraster falcatus*	1 L; S5 A-B	
Tokumm	2018-0507	65083			*Cambroraster falcatus*	2 F-H; S6	Paratype
Tokumm	2018-0508	65084			*Cambroraster falcatus*	2 A,B	Paratype
Tokumm	2018-0914	65085			*Cambroraster falcatus*	2 D	
Tokumm	2018-0685	65086			*Cambroraster falcatus*	2 J	
Tokumm	2018-0156	65087			*Cambroraster falcatus*	2 I	
Tokumm	2018-0373	65088			*Cambroraster falcatus*	S1 A,B	
Tokumm	2018-0493	65089			*Cambroraster falcatus*	S1 F,I	
Tokumm	2016-0657	65090			*Cambroraster falcatus*	S1 C,D	
Tokumm	2018-0492	65091			*Cambroraster falcatus*	S1 G,H	
Tokumm	2018-0849	65092			*Cambroraster falcatus*	1 M	Paratype
Tokumm	2018-0639	65313			*Cambroraster falcatus*	S4 A	
Tokumm	2018-0604	65314			*Cambroraster falcatus*	S4 B	
Tokumm	2018-0948	65315			*Cambroraster falcatus*	S4 C	
Tokumm	2018-0938	65316			*Cambroraster falcatus*	S7 C	
Collins Quarry	1988-0098	59255			*Hurdia*	3 A	

Fossil Ridge (EZ)							
Raymond Quarry	1997-0805	60048			*Hurdia*	3 E,F	
Raymond Quarry	1993-0165	65094			*Hurdia*	3 G	
Phyllopod Bed				274141	*Peytoia*	3 C	
Walcott Talus	2000-0824	61127			*Peytoia*	3 B	
Stanley Glacier	2008-0128	59944			*Stanleycaris*	3 H	
Chengjiang			162519		*Zhenghecaris*	S7 A	
Chengjiang			162520		*Zhenghecaris*	S7 B	
Raymond Quarry	1992-0601	51213			*Anomalocaris*	S8 A-E	
Raymond Quarry	1993-0269	61668			*Anomalocaris*	3 D; S8 G-H	
Raymond Quarry	1992-0489	61669			*Anomalocaris*	S8 F	

ROM Invertebrate Palaeontology - *Cambroraster* All Specimens List

Locality	**Field No.**	**Notes**	**Stratigraphic Level**
Marble Canyon	2014-0421	frontal appendage; P-element?	-138 cm
Marble Canyon	2014-1060	H-element with soft tissue? and P-element	-404 cm
Marble Canyon	2014-1221	complete body	-427 cm
Marble Canyon	2016-0999	H-element, fragment (just spines)	-353 cm
Mount Field (FM)	1984-1058	H-element, burrowed	Talus
Mount Stephen (WS)	1983-0227	H-element, partial	91.4 cm
Tokumm	2014-0163	H-element; one of the biggest	Talus
Tokumm	2014-0291	frontal appendage, spine	Talus
Tokumm	2014-0314	complete body	Talus
Tokumm	2016-0315	H-element	Talus
Tokumm	2016-0400	H-element	Talus
Tokumm	2016-0442	H-element; fragmentary	Talus
Tokumm	2016-0443	H-element	Talus
Tokumm	2016-0469	H-element; oblique view	Talus
Tokumm	2016-0493	H-element; frontal appendages	Talus
Tokumm	2016-0507	H-element	Talus
Tokumm	2016-0592	H-element x2	Talus
Tokumm	2016-0614	H-element in oblique view; possible body fragments	Talus

Tokumm	2016-0618	H-element fragment; frontal appendage	Talus
Tokumm	2016-0623	H-element; nice lateral spines	Talus
Tokumm	2016-0636	H-element; burrowed	Talus
Tokumm	2016-0638	H-element	-440 cm
Tokumm	2016-0640	H-element with P-elements in place?; body fragments?	Talus
Tokumm	2016-0645	H-element; frontal appendage	Talus
Tokumm	2016-0650	H-element, fragment	Talus
Tokumm	2016-0657	disarticulated assemblage: H-element, frontal appendages, flaps, oral plates	Talus
Tokumm	2016-0701	H-element with nice spines; frontal appendage; partial body?	Talus
Tokumm	2018-0032	frontal appendage, large	In situ
Tokumm	2018-0156	frontal appendages; oral cone	In situ
Tokumm	2018-0336	H-element	In situ
Tokumm	2018-0373	H-element; articulated body, weathered	Talus
Tokumm	2018-0395	H-element x2; frontal appendages	-480 cm
Tokumm	2018-0400	H-element, fragments	-480 cm
Tokumm	2018-0405	H-element; frontal appendages	-480 cm
Tokumm	2018-0424	frontal appendage, large endite	-470 cm
Tokumm	2018-0467	H-element; burrowed	-415 cm
Tokumm	2018-0469	H-element; burrowed	-409 cm
Tokumm	2018-0472	frontal appendage, large endite	-442 cm
Tokumm	2018-0492	H-element; frontal appendages; body parts	-465 cm
Tokumm	2018-0493	disarticulated assemblage: H-element, frontal appendages, body parts?	-465 cm
Tokumm	2018-0507	frontal appendages; oral cone	-470 cm
Tokumm	2018-0508	frontal appendage; excellent	-470 cm
Tokumm	2018-0521	H-element; frontal appendages; body parts?	-450 cm
Tokumm	2018-0522	H-element, fragments; frontal appendage	-470 cm
Tokumm	2018-0561	frontal appendage, nice, some disarticulated spines	-457 cm
Tokumm	2018-0586	disarticulated assemblage: H- and P-elements	-450 cm
Tokumm	2018-0595	frontal appendage, endite	-456 cm
Tokumm	2018-0601	H-element; frontal appendages	-365 cm
Tokumm	2018-0602	H-element	-433 cm
Tokumm	2018-0604	H-element x2; frontal appendage	-367 cm
Tokumm	2018-0610	H-element	-370 cm
Tokumm	2018-0612	H-element	-439 cm
Tokumm	2018-0628	H-element; frontal appendage x3	-428 cm
Tokumm	2018-0638	H-elements x2	-456 cm
Tokumm	2018-0640	frontal appendage, endites	-460 cm
Tokumm	2018-0644	frontal appendage, endites	No level
Tokumm	2018-0650	H-element x3; P-elements	-473 cm
Tokumm	2018-0657	H-element; frontal appendage	-438 cm

Tokumm	2018-0659	frontal appendage, endite	-460 cm
Tokumm	2018-0661	frontal appendage, endites	-462 cm
Tokumm	2018-0667	H-element, fragment; frontal appendage, endites	-466 cm
Tokumm	2018-0670	H-element fragment; frontal appendage, partial x3	-463 cm
Tokumm	2018-0679	H-element	-468 cm
Tokumm	2018-0685	oral cone	-446 cm
Tokumm	2018-0693	H-element x2	-445 cm
Tokumm	2018-0712	H-element	-475 cm
Tokumm	2018-0747	H-element, large	-470 cm
Tokumm	2018-0760	frontal appendages	-456 cm
Tokumm	2018-0763	fragmentary remains	-463 cm
Tokumm	2018-0766	disarticulated assemblage, fragmentary	-467 cm
Tokumm	2018-0779	frontal appendage, endite	-473 cm
Tokumm	2018-0781	frontal appendages, several disarticulated at different angles	-475 cm
Tokumm	2018-0791	disarticulated assemblages, several individuals	-475 cm
Tokumm	2018-0795	H-element, nice ornamentation	-469 cm
Tokumm	2018-0797	H-element	-470 cm
Tokumm	2018-0798	H-element	-475 cm
Tokumm	2018-0799	H-element	-454 cm
Tokumm	2018-0836	endites	-446 cm
Tokumm	2018-0838	H-element, large, poorly preserved	-457 cm
Tokumm	2018-0839	H-element, large, poorly preserved	-478 cm
Tokumm	2018-0843	H-element	-478 cm
Tokumm	2018-0856	H-element	-478 cm
Tokumm	2018-0861	H-element, partial	Talus
Tokumm	2018-0874	H-element	-475 cm
Tokumm	2018-0877	H-element, fragment; endites	-461 cm
Tokumm	2018-0879	H-element	No level
Tokumm	2018-0880	H-element	-465 cm
Tokumm	2018-0898	H element	-455 cm
Tokumm	2018-0899	frontal appendages x3; H-element fragments	-475 cm
Tokumm	2018-0901	H-element x2, large	No level
Tokumm	2018-0902	H-element, large	-470 cm
Tokumm	2018-0903	H-element x4; frontal appendages, disarticulated	-480 cm
Tokumm	2018-0912	mass moult assemblage	-478 cm
Tokumm	2018-0920	H-element, fragments	-480 cm
Tokumm	2018-0922	H-element, large x2	-465 cm
Tokumm	2018-0925	H-element	-477 cm
Tokumm	2018-0926	H-element	No level
Tokumm	2018-0938	H-element	-469 cm
Tokumm	2018-0941	H-element	-469 cm
Tokumm	2018-0942	H-element	-433 cm
Tokumm	2018-0948	H-element	-476 cm

Tokumm	2018-0950	H-element	-470 cm
Tokumm	2018-0951	H element; other body fragments?	-476 cm
Tokumm	2018-0952	H element x2	-470 cm
Tokumm	2018-0954	endites	-473 cm
Tokumm	2018-0964	disarticulated assemblage: H-, P-elements, frontal appendages, oral cone	-403 cm
Tokumm	2018-0965	H-element x2, nice spines	-450 cm
Tokumm	2018-0967	H-element; frontal appendages, fragmentary	-474 cm